Dissection of U4 snRNA Functional Domains Using *in Vitro* Reconstitution

Amy Hayduk

B. Sc., University of Northern British Columbia, 2006

Thesis Submitted in Partial Fulfillment of

The Requirements for the Degree of

Master of Science

In

Mathematical, Computer, and Physical Sciences

(Chemistry)

The University of Northern British Columbia

July 2009

Your file Votre référence
ISBN: 978-0-494-60840-1
Our file Notre référence
ISBN: 978-0-494-60840-1

Abstract

Splicing, the removal of non-protein-coding introns from pre-mRNA, is a critical step in eukaryotic gene expression. Splicing is catalyzed by the spliceosome, which is composed of five small nuclear RNAs (U1, U2, U4, U5, and U6) and over 100 proteins. To facilitate molecular dissection of the structure and function of U4, we have developed an *in vitro* assay for reconstitution of functional U4 snRNPs. Depletion of U4 strongly inhibited splicing, and subsequent addition of wild-type *in vitro* transcribed U4 allowed efficient recovery of splicing. Analysis of reconstitution by U4 3′ truncation mutants showed that, while the Sm protein binding site was dispensable for splicing *in vitro,* shorter mutants lacking the 3′ stem-loop were unable to reconstitute splicing. We showed that the 3′ stem-loop was essential for formation of the yeast di-snRNP, but it was dispensable for subsequent steps of spliceosome assembly and splicing.

TABLE OF CONTENTS

List of Figures

Acknowledgement

Firstly, I would like to thank my family for their support throughout my academic endeavors, and for at least trying to understand what it is that I do in the lab all day! I would also like to thank my supervisor, Dr. Stephen Rader, and committee members, Drs. Cecilia Alstrom-Rapaport and Dezene Huber, for their guidance and encouragement during the completion of my Masters thesis. I am deeply grateful to Drs. Martha Stark and Kelly Aukema for their invaluable mentorship and technical assistance, as well as to all the members of the Rader lab for helpful discussions throughout this project. Finally, I would like to acknowledge the financial support provided by the Natural Sciences and Engineering Research Council of Canada, the Michael Smith Foundation for Health Research, and UNBC.

CHAPTER 1

Introduction

1.1 Gene Expression

Proteins play an incredibly diverse range of structural and functional roles in the physiology of all living organisms. These include acting as the enzymes that catalyze nearly all chemical reactions that occur in a cell; acting as hormones involved in communication between cells; and functioning as integral parts of the immune system. Given this extensive array of functions, it is clear that expression of any given protein may only be required in certain cell types or at certain times of development. It is also energetically expensive to produce proteins. Consequently, proteins are only produced when and where they are required.

The instructions for producing proteins are encoded in genes in the DNA, which in eukaryotic organisms is found within the nucleus. When the protein product of a specific gene is required, an RNA copy of the gene, called precursor messenger RNA (pre-mRNA), is generated through transcription. This gene copy undergoes a number of processing events, including 5′ cap formation and addition of a polyadenosine tail, before it is exported to the cytoplasm where it directs protein synthesis through interaction with the ribosome during translation.

1.2 Pre-mRNA Splicing

A feature of nearly all eukaryotic genes is that they are interrupted by sequences that do not code for protein. These intervening sequences, or introns, are included in the RNA copy of the gene and therefore must be removed from the pre-mRNA before it can be used to

direct protein synthesis. The process of removing introns from the pre-mRNA and reconnecting the flanking coding sequences, or exons, to form mature mRNA is known as pre-mRNA splicing. Although it has been more than 30 years since the discovery of introns within the coding sequences of genes (Berget et al. 1977, Chow et al. 1977), scientists are still far from fully understanding the splicing process due to its complexity.

Splicing is guided by three conserved regions of the pre-mRNA transcript: the 5′ and 3′ splice sites (ss), which mark the intron boundaries, and the branch point sequence, which is found upstream of the 3′ss and contains an important adenosine residue (Figure 1). The 5′ and 3′ boundaries of an intron are defined by a GU and an AG dinucleotide, respectively, more than 99% of the time (Burset et al. 2000, Black 2003). The small number of remaining introns are defined by non-canonical sequences (Burset et al. 2000). These elements of the pre-mRNA are central to the two transesterification reactions by which splicing is accomplished.

In the first step of splicing, the phosphate at the 5′ splice site undergoes nucleophilic attack by the free 2′ hydroxyl of the branch point adenosine, freeing the 5′ exon. The 3′ exon remains attached to the intron, which assumes a lariat configuration due to formation of a 2′-to-5′ phosphodiester bond between the branch point adenosine and the 5′ end of the intron. In the second reaction, nucleophilic attack of the 3′ splice site by the 3′ hydroxyl of the 5′ exon joins the two exons, producing mature mRNA and releasing the intron lariat (Figure 1).

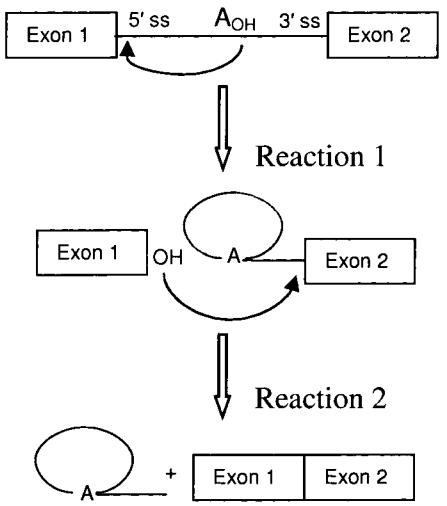

Figure 1. The two chemical reactions of pre-mRNA splicing. The intron is represented by a black line and the branch point adenosine by A_{OH}.

The process of splicing is made more complex by the presence of multiple introns in a single pre-mRNA transcript. Such transcripts require multiple splicing events for formation of mature mRNA, and, through alternative splicing, allow for production of numerous protein isoforms from a singe gene (reviewed in Black 2003). Alternative splicing is a major contributor to the protein diversity of higher eukaryotes. In humans, for example, it is estimated that alternative splicing plays a role in expression of over 70% of genes (Johnson *et al.* 2003). Thus, the approximately 22,000 genes of the human genome to encode an estimated 90,000 proteins, helping to explain the complexity of humans relative to much simpler organisms possessing a comparable number of genes (Harrison 2002).

1.3 Splicing and Disease

Given the central role of splicing in gene expression and the single-nucleotide accuracy of splice site recognition required to produce the correct protein, it is not surprising

that many diseases stem from errors in splicing. In fact, it has been estimated that approximately half of all human genetic diseases are the result of mutations which affect splicing (Buratti *et al.* 2006, Lopez-Bigas *et al.* 2005). These include spinal muscular atrophy, which is one of the most common causes of childhood mortality; a group of eye conditions known as retinitis pigmentosa, which ultimately result in blindness; and neurodegenerative diseases such as Alzheimer's and Parkinson's diseases. Mutations in splicing have also been linked to cystic fibrosis, myotonic dystrophy, and a large number of cancers (Faustino and Cooper 2003). The ultimate discovery of cures for such diseases is closely tied to determining their molecular origins.

1.4 Yeast as a Model Organism

Although the ultimate goal of pre-mRNA splicing studies is to elucidate the mechanism by which this fundamental process occurs in our own bodies, many of these studies are carried out in yeast (*Saccharomyces cerevisiae*). There are a number of reasons why yeast is an attractive model organism for biochemical studies, and for splicing studies in particular. First, yeast has been the subject of intense genetic analysis for over a century, resulting in the availability of a vast array of genetic tools and mutant strains (Miesfeld 1999). Furthermore, many biochemical tools and techniques are available for yeast, including a well-established protocol for *in vitro* splicing that has proved invaluable to investigations of the effects of genetic modifications on splicing (Lin *et al.* 1985). Second, yeast is a eukaryotic system which is considerably less complex than other eukaryotic systems, such as the mammalian cell. The yeast genome, at twelve million DNA base-pairs, is 250 times smaller than the three billion-base-pair human genome. The relative simplicity of the yeast

genome allowed for its complete sequencing by 1996 (Goffeau *et al.* 1996), which had an enormous impact on yeast research. Genomic sequencing has revealed that, of the approximately 6000 genes found in yeast (Goffeau *et al.* 1996), only about 250 of them, or less than 5%, contain an intron (Davis *et al.* 2000). In comparison, over 95% of human genes contain an intron (Lander *et al.* 2001). Study of splicing in yeast is further enhanced by the fact that the vast majority of intron-containing genes in yeast possess only a single intron (SGD Project 1997), eliminating interference from alternative splicing. Finally, a large number of genes are evolutionarily conserved between yeast and humans (Miesfeld 1999). For example, among splicing-related molecules, the protein Prp8 is 62% identical between yeast and humans (Luo *et al.* 1999) and the catalytically important central domain of U6 RNA is 80% identical (Guthrie and Patterson 1988, Brow and Guthrie 1989). The high degree of conservation of splicing components and mechanism between these organisms means that details of the splicing process obtained from yeast research are highly relevant to our understanding of this process in humans (Rymond and Rosbash 1992).

1.5 The Spliceosome and the Splicing Cycle

The average human gene contains eight exons, each approximately 145 nucleotides in length (Lander *et al.* 2001). These coding sequences are distinguished from the surrounding introns, which average more than ten times the length of an exon (Lander *et al.* 2001), by relatively short, degenerate 5′ and 3′ ss sequences. The task of recognizing these genetic signals and thereby discriminating between exon and intron belongs to a dynamic macromolecular complex called the spliceosome.

The spliceosome is an enzymatic ribonucleoprotein complex containing five different small nuclear RNAs (snRNAs) that are particularly rich in uridine residues and are thus known as U1, U2, U4, U5, and U6. Each of these RNAs interacts with a number of proteins to form the associated small nuclear ribonucleoprotein particle (snRNP). Through a highly orchestrated series of interactions with each other and the pre-mRNA, these snRNPs modify the original gene transcript en route to its becoming mature mRNA ready to undergo translation.

The primary interaction between the splicing machinery and the pre-mRNA occurs between the U1 snRNP and the 5′ ss (Figure 2), forming the E complex or commitment complex. Subsequently, the U2 snRNP forms a base-pairing interaction with the branch point, assisted by an assembly of branch point-binding proteins, forming the B complex or pre-spliceosome. This is followed by participation of the U4/U6•U5 tri-snRNP, which consists of extensively base-paired U4 and U6 snRNPs in association with the U5 snRNP, forming the A complex (reviewed in Nilsen 1994, Staley and Guthrie 1998).

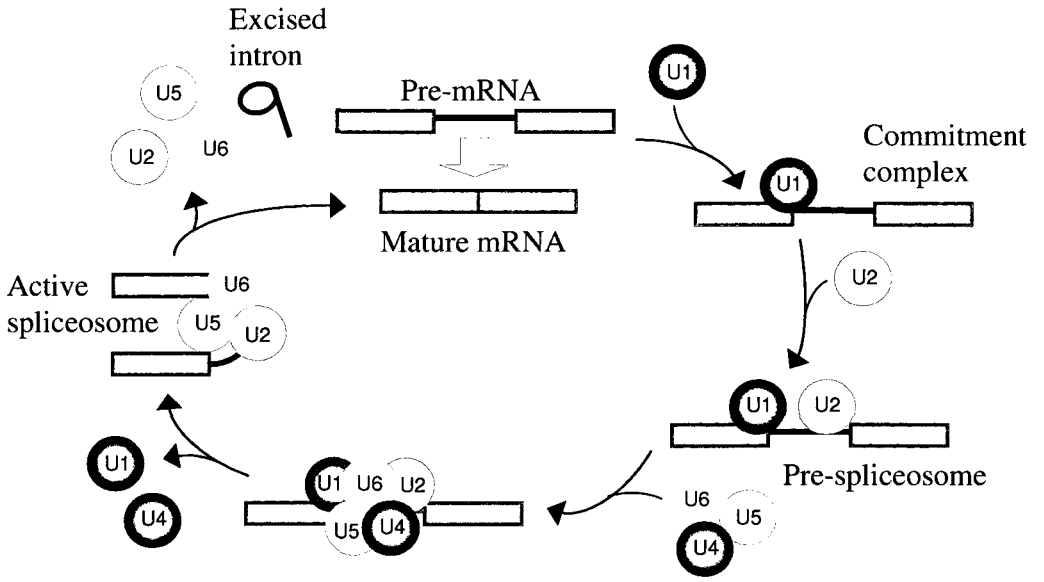

Figure 2. The cycle of snRNP assembly complexes involved in pre-mRNA splicing. The red arrow indicates the overall result of intron removal.

The interactions of these five snRNPs with each other and the pre-mRNA substrate are highly dynamic. Following entrance of the tri-snRNP, a number of rearrangements occur within the A complex that cause it to become catalytically active. These rearrangements are assisted by a family of ATP-dependent RNA unwindases known as the DEAD/DEXH-box proteins (Staley and Guthrie 1998). Binding of U1 at the 5′ ss is replaced by U6, and base-pairing between U4 and U6 is disrupted to allow formation of mutually exclusive structures involving an interaction between U2 and U6 (Madhani and Guthrie 1992) and a U6 intramolecular stem-loop that coordinates a metal ion important for 5′ ss cleavage (Yean *et al.* 2000, Huppler *et al.* 2002). The result of these exchanges is the destabilization or release of U1 and U4 from the spliceosome, leaving U2 and U6 bound to the branch point and 5′ ss, respectively, with U5 interacting with the two exons. This arrangement of U2, U5, and U6 assembled on the pre-mRNA is termed the active spliceosome (Figure 2), and it is this set of components that actually catalyzes the two chemical steps of splicing. Once the splicing

reaction is complete, the excised intron is degraded and the snRNPs are returned to their original conformations to be recycled through future rounds of splicing (Staley and Guthrie 1998).

1.6 The Role of the U4 snRNP in Splicing

1.6.1 Current Understanding

While the general roles of U1, U2, U5, and U6 in the splicing process are at least reasonably well understood, the function of U4, though essential for splicing (Berget and Robberson 1986, Black and Steitz 1986, Siliciano *et al.* 1987, Brow and Guthrie 1988), is not. Like U1, U4 is not directly involved in catalysis of splicing, as it is thought to exit the spliceosome prior to the first chemical reaction (Pikielny *et al.* 1986, Cheng and Abelson 1987, Lamond *et al.* 1988, Yean and Lin 1991). However, unlike U1, U4 is not known to form any contacts with the pre-mRNA, although cross-linking studies have demonstrated that U4 is in close proximity to the 5′ ss at early stages of spliceosome assembly (Johnson and Abelson 2001).

It is known that U4 forms an extensive and stable base-pairing interaction with U6 through intermolecular stems I and II (Figure 3a; Brow and Guthrie 1988, Guthrie and Patterson 1988). Formation of the U4/U6 base-pairing interaction is catalyzed by the splicing factor Prp24 (Ghetti *et al.* 1995, Raghunathan and Guthrie 1998). The mechanism for formation of this duplex is not known, though it has been suggested to occur through a so-called kissing-loop interaction (Figure 3b) (Karaduman *et* al. 2006; Ollenberger and Rader, unpublished results). Furthermore, the function of this U4/U6 interaction has yet to be established.

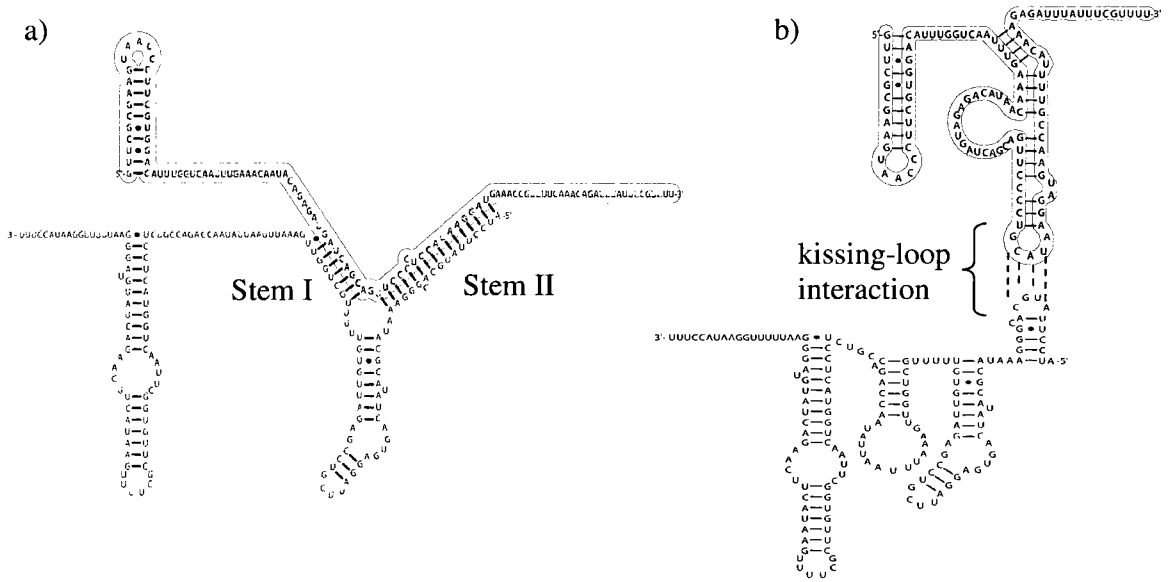

Figure 3. Secondary structures of the U4 (yellow) and U6 (red) snRNAs. a) The U4/U6 di-snRNA containing intermolecular stems I and II. b) Potential mechanism of initiation of base-pairing between free U4 and U6 snRNAs.

One hypothesis is that the U4/U6 interaction allows U4 to function as a negative regulator of U6 activity. Prior to the first catalytic step of the splicing reaction, U6 must undergo a remarkable series of rearrangements in which base-pairing between U4 and U6 is broken to allow U6 to form mutually exclusive interactions with U2 and the 5′ ss (Figure 4, Umen and Guthrie 1995). It has therefore been proposed that U4 may prevent premature rearrangements of U6 by holding it in an inactive conformation through sequestration of its catalytic residues (Guthrie and Patterson 1988, Brow and Guthrie 1989). Disruption of the U4/U6 interaction and release of U4 from the spliceosome would then act as a switch for spliceosome activation, and factors that stabilize or destabilize the U4/U6 interaction would regulate this activation (Murray and Jarrell 1999). However, given that yeast cells contain a large molar excess of U6 over U4 (Li and Brow 1993), and that these molecules are thought to interact in a one-to-one manner (Hashimoto and Steitz 1984, Rinke *et al.* 1985, Brow and

Guthrie 1988, Bindereif *et al.* 1990), it is not plausible that U4 acts as a negative regulator of a molecule so much more abundant than itself.

A second hypothesis is that U4 instead acts as an activator of splicing. It is clear that interaction between U4 and U6 is required for incorporation of the latter into the spliceosome (Brow and Guthrie 1988, Staley and Guthrie 1998). This observation has led to the suggestion that U4 may activate U6 by holding it in a favorable conformation for interaction with the pre-mRNA (McConnell and Steitz 2001). Although the mechanistic explanation for this activation is unknown, it is an attractive proposal since it is more consistent with the relative levels of U4 and U6 found in yeast cells (Li and Brow 1993). In fact, these two hypotheses regarding the function of U4 may not be mutually exclusive; U4 may initially act as an activator to allow U6 to enter the spliceosome, where it may then adopt a negative regulatory role, preventing the conformational changes required for progression to the active spliceosome until the correct base-pairing between U6 and the 5′ ss has been established.

1.6.2 Structural Basis for a Role of U4 in Spliceosome Activation

As the function of each snRNP is intimately linked to its structure, elucidation of these structures provides important insights into the splicing mechanism. Although an activating role for U4 in spliceosome assembly seems reasonable, evaluation of this possibility has been hindered by lack of a structural model of free U6 prior to its interaction with U4 that could explain such an activating effect. While a number of structural models of free U6 have been proposed (Fortner *et al.* 1994, Ryan *et al.* 2002, Karaduman *et al.* 2006), none are entirely consistent with existing structure probing data or the known interactions of U6. However, the Rader Lab has recently proposed a new model for the structure of free U6

that addresses a significant number of the shortcomings of existing models (Dunn and Rader, unpublished). A key feature of this model is the prediction of a molecular mechanism by which the U4/U6 interaction could allow U6 to enter the spliceosome (Figure 4), something that previous models did not incorporate. Specifically, in contrast to previous U6 models, a catalytically important region of U6, the ACAGAGA sequence, is suggested to be sequestered in the Dunn-Rader model (Figure 4), preventing premature interaction with the pre-mRNA. Formation of the U4/U6 di-snRNP frees this sequence, thus activating U6 for participation in spliceosome assembly and splicing (Figure 4).

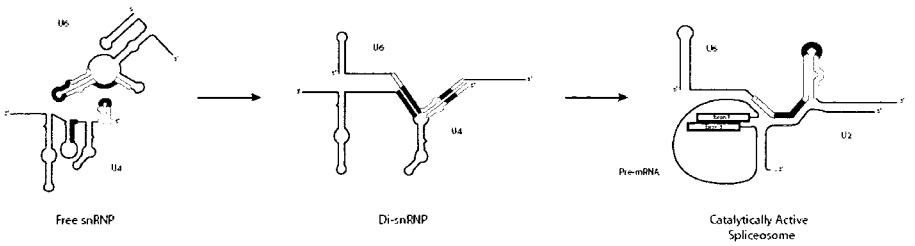

Figure 4. Model for activation of U6 through interaction with U4. The catalytically important ACAGAGA sequence of U6 (red), sequestered in the free snRNP (left), is exposed through formation of the U4/U6 di-snRNP (middle), allowing subsequent interaction with the 5′ splice site of the pre-mRNA (right).

Further examination of the role of U4 in splicing is necessary to determine whether U4 does in fact function as an activator of U6. One approach to examine such a role in activation is to identify the minimum U4 sequence required for di-snRNP formation and subsequent interaction of U6 with the pre-mRNA, and to determine whether this sequence is consistent with the U6-activating sequence, U4 stem II, predicted by the Dunn-Rader model of U6. These studies would benefit significantly from availability of a yeast system enabling *in vitro* reconstitution of functional U4 snRNPs.

1.7 *In Vitro* Splicing Reconstitution

In vitro reconstitution assays are powerful tools for molecular dissection of biological processes. Splicing reconstitution assays are particularly useful for identifying essential constituents of the reaction and can provide important insights into the interactions, structure, and function of molecules involved in splicing. These assays involve depletion of a specific component of the splicing machinery from cell extract to abolish splicing activity, followed by complementation with a modified version of that component to allow examination of the effects of certain mutations on splicing activity or to investigate the interactions formed by that component (Newman 1994).

A number of early studies demonstrating *in vitro* reconstitution of all five mammalian snRNPs have identified snRNA domains required for snRNP assembly (Hamm *et al.* 1987, 1989, Patton *et al.* 1987, Riedel *et al.* 1987, Patton and Perderson 1988, Kleinschmidt *et al.* 1989, Pikielny *et al.* 1989, Bindereif *et al.* 1990, Wersig and Bindereif 1990, Sumpter *et al.* 1992). Importantly, these *in vitro*-assembled snRNPs have been shown to be active in splicing (Wersig and Bindereif 1992, Wolff and Bindereif 1992, Segault *et al.* 1995, Will *et al.* 1996). Similar *in vitro* splicing reconstitution systems have been developed for yeast U2, U5, and U6 (Fabrizio *et al.* 1989, McPheeters *et al.* 1989, O'Keefe *et al.* 1996), although there has been no report of reconstitution analyses of yeast U1 or U4. Together, these splicing reconstitution assays have facilitated numerous analyses of snRNP function and have allowed elucidation of snRNA functional domains and their protein interaction partners (Fabrizio and Abelson 1990, Wolff *et al.* 1994, Dix *et al.* 1998, O'Keefe and Newman 1998, Vidal *et al.* 1999, Alvi *et al.* 2001, McGrail *et al.* 2006).

Considering specifically the human U4 snRNA, *in vitro* reconstitution with a variety of deletion mutants has enabled dissection of the functional domains of this molecule and has revealed the roles of these regions in snRNP and spliceosome assembly and splicing activity (Wersig and Bindereif 1990, 1992). These studies have shown that, while the 5′ portion of U4 is necessary for U4/U6 interaction, spliceosome assembly, and splicing, the 3′ portion of the molecule appears nonessential (Wersig and Bindereif 1990, 1992). Within the 5′ region, only stem II was found to be essential for splicing, though deletion of either stem I or the intervening 5′ stem-loop also resulted in a significant reduction of splicing activity (Wersig and Bindereif 1992). Similarly, stem II was found to be essential for U4/U6 interaction, while a stem I deletion mutant exhibited significantly reduced binding to U6 (Wersig and Bindereif 1990).

While these *in vitro* reconstitution analyses have provided important insights into the domain structure of U4, many questions remain regarding the identity of the functionally important nucleotides within these domains, as well as the specific points in the splicing cycle at which they act. Furthermore, we have only a limited knowledge of the identities of the proteins associated with U4 snRNA, the sequences with which they interact, and the roles they may perform during snRNP and spliceosome assembly and splicing catalysis. Given the vast array of biochemical and genetic tools and techniques offered by yeast, investigation of these questions would be greatly facilitated by the availability of a system for reconstitution of functional U4 snRNPs in this organism.

1.8 Overall Research Objective

Despite being an essential component of the pre-mRNA splicing reaction, yeast U4 snRNA remains largely uncharacterized with respect to its domain structure, the proteins with which is associates, and its function. A valuable tool to address these questions would be an assay for *in vitro* reconstitution of functional U4 snRNPs, such as has been highly useful in structural and functional analyses of other snRNAs. Accordingly, the aim of the research project presented here was to develop a yeast U4 *in vitro* reconstitution system that could then be used to investigate the minimum U4 sequence required for snRNP formation, spliceosome assembly, and splicing; whether this sequence is consistent with the predictions of the Dunn-Rader model for the structure of free U6; and finally, whether formation of the U4/U6 duplex is initiated through a kissing-loop interaction.

CHAPTER 2

Identification of Optimal Conditions for U4 Degradation and Splicing Inhibition

Development of an *in vitro* assay for reconstitution of functional U4 snRNPs requires removal of endogenous U4 from the extract, blocking splicing activity. The extract can then be used to examine the activities of mutant versions of U4. To deplete endogenous U4 from yeast splicing extract, I used oligonucleotide-directed degradation by RNase H. I considered several factors in the design of the RNase H degradation reaction, including concentrations of DNA oligonucleotide, enzyme, and ATP, incubation time, and reaction temperature. The limits of these parameters are defined, to some extent, by downstream functional studies of the depleted extract, namely snRNP and spliceosome assembly, and ultimately, splicing activity. Therefore, I examined a range of conditions to balance degradation efficiency with maintenance of splicing extract activity. I identified conditions that allowed efficient depletion of full-length U4 from yeast extract, effectively blocking spliceosome assembly and splicing.

2.1 Materials and Methods

2.1.1 Splicing Extract Preparation

Whole-cell extract was prepared from protease-deficient yeast strain BJ2168 as previously described (Ansari and Schwer 1995). Frozen cell pellets were homogenized to a very fine powder using a mortar and pestle.

2.1.2 Oligonucleotide-Directed RNase H Degradation of U4

RNase H degradation reactions contained 60mM KPO_4, 2.5mM $MgCl_2$, 3% PEG 8000, 50% splicing extract, 2mM ATP (unless otherwise stated), 2 units RNase H (unless

otherwise stated) (Ambion), the indicated concentrations or amounts of targeting oligonucleotide and unlabeled IVT actin pre-mRNA, and dH_2O to 8μL. DNA targeting oligonucleotides used were

JPS151 (complementary to U4 nucleotides 1 to 19)

5' ATTTCCCGTGCATAAGGAT 3'

SDR553 (complementary to U4 nucleotides 1 to 30)

5' CTGATATGCGTATTTCCCGTGCATAAGGAT 3'

Reactions were incubated for 30 minutes (unless otherwise indicated) at 23, 30, or 37°C, as indicated in the figures.

2.1.3 Northern Blot Analysis of U4 Degradation

I added 200μL stop solution (0.3M NaOAc, 1mM EDTA, 0.1% SDS, 34μg/mL E. coli tRNA) to each 8μL RNase H reaction, followed by 200μL low-pH phenol:cholorform:isoamyl alcohol (25:24:1). Reactions were mixed by inversion, incubated at 65°C for five minutes, and spun at 13.2 krpm for five minutes. 170μL of the aqueous layer was removed to a new eppendorf tube, mixed by inversion with 200μL chloroform, and spun at 13.2 rpm for one minute. 150μL of the aqueous layer was removed to a new eppendorf tube and mixed by inversion with 40μg glycogen and 800μL cold 100% ethanol. Tubes were spun at 13.2 krpm for 30 minutes to precipitate the RNA. Pellets were washed with 70μL cold 70% ethanol and resuspended in 8μL 7M urea loading buffer. Samples were electrophoresed through a 6% 7M urea denaturing polyacrylamide gel at 400V for 30

minutes. RNA was transferred to a membrane by electroblotting at 450mA for 15 minutes followed by UV cross-linking. The membrane was then probed using ^{32}P-labeled U4 14B oligonucleotide complementary to the 3' end of U4 and exposed to a phosphor screen.

To calculate degradation efficiency, autoradiograms were visualized and quantified using a Cyclone© phosphoimager and Optiquant© software (Packard Instruments). U4 degradation efficiency was calculated by dividing the intensity of the full-length U4 band of each degradation reaction by the intensity of the same band in the mock degradation reaction (lacking targeting oligonucleotide) and subtracting this value from one.

2.1.4 Pre-mRNA Splicing Assay

To assess the effect of U4 degradation on splicing activity, I added 1μL ^{32}P-labeled actin pre-mRNA (4 fmol) to the extract subsequent to the RNase H reaction and incubated the reaction at 23°C for 30 minutes. Splicing controls contained 60mM KPO_4, 2.5mM $MgCl_2$, 3% PEG 8000, 2mM ATP, and 50% splicing extract in 8μL. Following addition of 1μL ^{32}P-labeled actin pre-mRNA (4 fmol), control reactions were incubated at 23°C for 30 minutes (positive control) or zero minutes (negative control). Splicing reactions were terminated by addition of 200μL stop solution, extracted with phenol:chloroform, and ethanol precipitated as described in section 2.1.3. Samples were electrophoresed through a 6% 7M urea denaturing polyacrylamide gel at 400V for one hour. The gel was then exposed to a phosphor screen at -80°C.

To calculate splicing efficiency, autoradiograms were visualized and quantified using a Cyclone© phosphoimager and Optiquant© software (Packard Instruments). Percent splicing was calculated by dividing the intensity of bands corresponding to product (mRNA and lariat) by the total intensity of all bands (pre-mRNA, lariat-3′ exon, 5′ exon, lariat, and

mRNA). Splicing inhibition was calculated by dividing the percent splicing of the depleted extract by that of the mock-depleted extract and subtracting this value from 1.

2.1.5 Spliceosome Assembly Gels

To assess the effect of U4 degradation on spliceosome assembly, 8μL aliquots of mock- or U4-depleted splicing extract were incubated with 1μL ^{32}P-labeled actin pre-mRNA (4 fmol) at 23°C for the indicated time before being adjusted to 0.7mg/mL heparin and 12% glycerol and run on a 1.5% agarose gel in 50mM tris/glycine buffer for 3.5 hours at 70V. The gel was dried and exposed to a phosphor screen for visualization.

2.2 Results and Discussion

2.2.1 Optimal Conditions for U4 Degradation

There has been a previous attempt to develop a yeast *in vitro* splicing reconstitution assay through RNase H degradation of U4, but it was not successful (Fabrizio and Abelson, unpublished results; Horowitz and Abelson 1993). In that study, a DNA oligonucleotide that targeted U4 nucleotides 72 to 92 was used, as it had been shown to direct nearly complete degradation of the target sequence (Xu *et al.* 1990). However, Fabrizio and Abelson (unpublished results) found that degradation of this central region of U4 failed to block splicing activity.

I, instead, targeted the 5′ end of U4, which has been shown to be essential for U4/U6 assembly and splicing (Vankan *et al.* 1990, 1992; Wersig and Bindereif 1990, 1992). Although Xu *et al.* (1990) found this region of yeast U4 to be almost entirely resistant to oligonucleotide-directed RNase H degradation, I found that it can be efficiently degraded by RNase H in reactions performed under conditions of active pre-mRNA splicing in which

snRNPs are being recycled for future rounds of splicing (Figure 5, lanes 4-7; Figure 8, lanes 5-8). The explanation for this observed increase in degradation of the 5′ end of U4 under splicing conditions is that, during spliceosome assembly, the U4 snRNP that entered the spliceosome base-paired to U6 is thought to be ejected from this complex as a free particle. In this free U4 species, the 5′ region that is normally engaged in base-pairing with U6 is believed to adopt a stem-loop conformation that is more accessible to the targeting DNA oligonucleotide (Figure 3). Titration of actin pre-mRNA showed that higher amounts of actin, and thus higher levels of splicing activity, allowed increased efficiency of U4 degradation (Figure 6). Addition of 20 fmol actin to the RNase H reaction resulted in nearly complete degradation of U4, while lower amounts of actin resulted in decreased U4 degradation (Figure 6).

While splicing extract contains factors that allow recycling of spliceosomal components for future rounds of splicing, the activity of these factors, and thus the number of splicing cycles that can be performed by a specific extract, is limited (Raghunathan and Guthrie, 1998). Therefore, it was important to ensure that the splicing performed during the RNase H reaction, while allowing increased U4 degradation, was not compromising the future splicing potential of the extract. Accordingly, I examined splicing in mock depleted extracts incubated with or without 20 fmol actin. Comparison of the splicing efficiencies of these extracts showed that the level of splicing that occurred during the RNase H reaction decreased the downstream splicing activity of the extract by less than 10% (Figure 10, lanes 1-4).

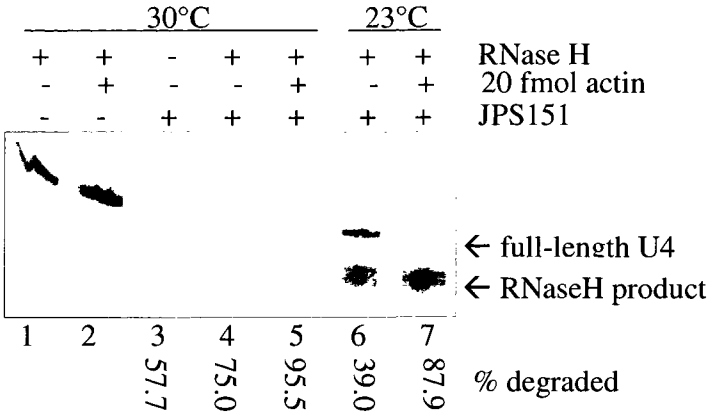

Figure 5. The 5′ end of U4 is more susceptible to RNaseH degradation under conditions of active splicing. Northern blot of U4 degradation in splicing extracts incubated at 30 or 23°C in the presence or absence of 2 units RNase H, 20 fmol actin pre-mRNA, and 10μM JPS151. U4 degradation efficiency is indicated below the gel.

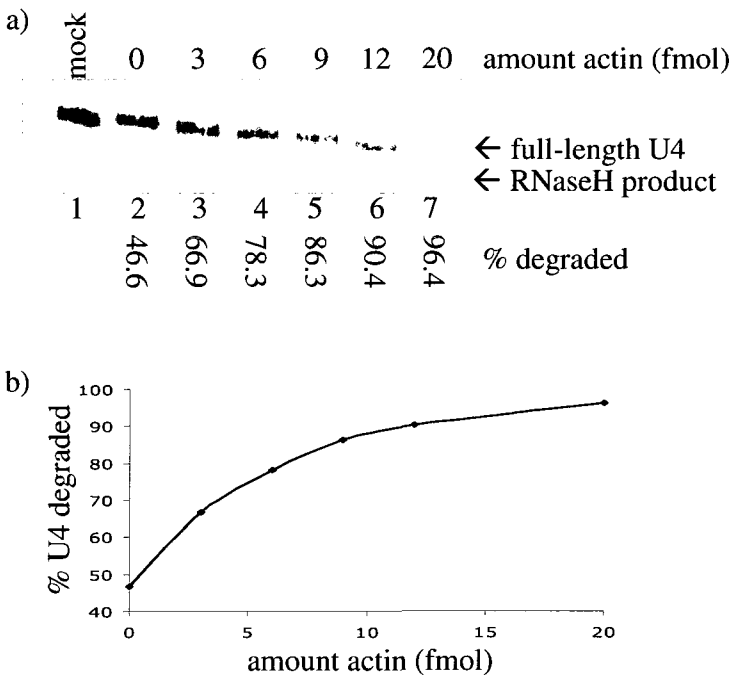

Figure 6. U4 degradation efficiency increases with the amount of actin pre-mRNA added to the reaction. a) Northern blot of U4 degradation in mock (lane 1) or U4-depleted splicing extract (lanes 2-7) in the presence of the indicated amounts of actin pre-mRNA. U4 degradation efficiency is indicated below the gel. b) Correlation between U4 degradation efficiency and the amount of actin pre-mRNA present in the reaction.

Enzyme concentration is also an important factor when optimizing depletion of an RNA molecule using RNase H. In depletion of yeast U2 and U6 snRNAs (McPheeters *et al.* 1989, Fabrizio *et al.* 1989), no exogenous RNase H was added because yeast splicing extract contains endogenous RNase H (Rymond and Rosbash 1986, Fabrizio *et al.* 1989, Newman 1994). However, it is often beneficial to supplement RNase H depletion reactions with additional enzyme (Lamond and Sproat 1994). Therefore, I examined U4 degradation in the absence and presence of 2 units exogenous RNaseH and found that addition of enzyme improved degradation efficiency from 57.7% to 75.0% (Figure 5, lanes 3 and 4). As addition of 6 units RNase H did not improve degradation efficiency any further (Figure 8, lane 10), 2 units RNase H was used in all remaining experiments presented in this section.

Incubation temperature and time were varied to identify conditions that yield optimal U4 depletion. As with the previously discussed reaction parameters, these variables had to be optimized to yield maximum degradation efficiency while still allowing robust splicing. For example, although the optimal incubation temperature for an RNase H degradation reaction is 37°C (manufacturer recommendation), splicing extract becomes inactivated at elevated temperatures (Lin *et al.* 1985). Therefore, I examined U4 degradation at three different incubation temperatures. As shown in Figures 5 (lanes 4-7), 7 (lanes 2 and 3), and 8 (lanes 5-8), 30°C resulted in better U4 degradation than 23°C. This was probably due to increased activity of the enzyme as it approached its optimal reaction temperature. However, degradation of U4 at the enzyme's optimal temperature of 37°C was actually less efficient than at 30°C (Figure 7, lanes 2 and 4). This was probably due to the fact that splicing activity, which, as shown above, is important for efficient U4 degradation, is maximal around room temperature and is inhibited at higher temperatures (Lin *et al.* 1985). Therefore, the

observed optimal temperature for U4 degradation of 30°C represents a balance of the optimal temperatures for both RNase H activity and splicing. I similarly examined the effect of incubation time on U4 degradation efficiency. As shown in Figure 8 (lanes 5 and 9), incubation of the RNase H reaction at 23°C for 3 hours did not result in better U4 degradation than incubation at 30°C for 30 minutes. Furthermore, although I did not examine the effect of such an extended incubation on the extract's splicing capacity, activity would probably have been decreased due to increased degradation and denaturation of spliceosomal components. Therefore, I incubated all subsequent RNase H reactions for 30 minutes at 30°C.

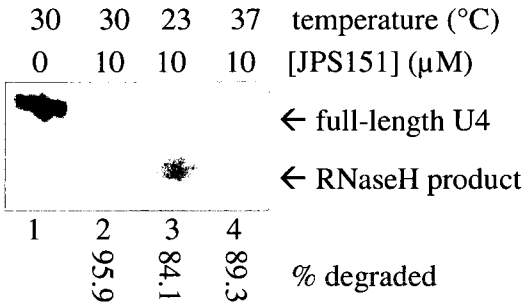

Figure 7. U4 degradation efficiency varies with the reaction temperature. Northern blot of U4 degradation in splicing extract incubated at 23, 30, or 37°C with the indicated concentrations of JPS151 and amounts of actin pre-mRNA. U4 degradation efficiency is indicated below the gel.

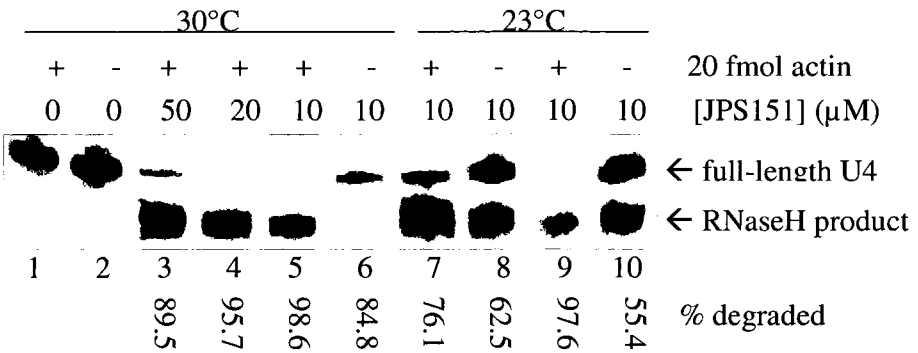

Figure 8. Effect of increased oligonucleotide concentration and incubation time on U4 degradation efficiency. Northern blot of U4 degradation in splicing extract incubated at 30°C or room temperature with the indicated concentrations of JPS151 in the presence or absence of 20 fmol actin pre-mRNA. The degradation reaction in lane 9 was incubated for 3 hours. The degradation reaction in lane 10 contained 6U RNase H. U4 degradation efficiency is indicated below the gel.

The concentration of targeting DNA oligonucleotide is a critical parameter in RNase H depletion reactions; too low a concentration results in incomplete degradation of the target RNA, while too high a concentration can lead to nonspecific degradation of other RNAs in the extract (Lamond and Sproat 1994) and can also inhibit downstream reconstitution of the targeted RNA species. Given that the optimal concentration of DNA oligonucleotide depends on degradation efficiency and therefore must be determined empirically, I assessed a range of oligonucleotide concentrations. As shown in Figure 8 (lanes 3-5), oligonucleotide concentrations above 10μM did not improve U4 degradation. However, examination of oligonucleotide concentrations below 10μM showed that maximum U4 degradation was achieved with 5μM oligonucleotide (Figure 9, lanes 5-7). This oligonucleotide concentration is approximately 10-fold higher than that used by McPheeters *et al.* (1989) and Fabrizio *et al.* (1989) in the degradation of yeast U2 and U6, respectively. The disparity between these values suggests a significant difference in the accessibilities of the regions of the snRNA molecules being targeted.

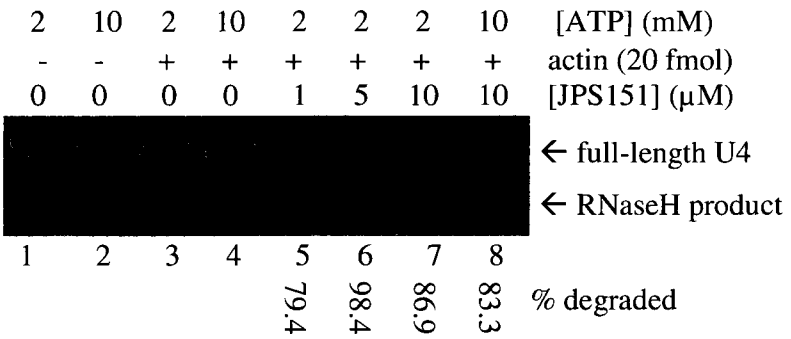

Figure 9. Effect of decreased oligonucleotide and increased ATP concentrations on U4 degradation efficiency. Northern blot of U4 degradation in splicing extract incubated with the indicated concentrations of ATP and oligo in the presence or absence of 20 fmol actin pre-mRNA. U4 degradation efficiency is indicated below the gel.

2.2.2 Inhibition of Spliceosome Assembly and Splicing by U4 Degradation

A critical consideration in the development of an *in vitro* splicing reconstitution assay through RNase H degradation of U4 is that degradation of endogenous U4 must inhibit the splicing activity of the extract. As mentioned above, a previous attempt to develop such a system was unsuccessful because degradation of the chosen target sequence within U4 did not block splicing (Fabrizio and Abelson, unpublished results; Horowitz and Abelson 1993). In my study, I targeted a different region of U4, the 5′ end, for degradation, resulting in efficient inhibition of splicing (Figure 10, lanes 5-8). Figure 11 shows that there is a close correlation between the fraction of U4 degraded in a splicing extract and inhibition of its splicing activity; 5 μM oligonucleotide provided the greatest U4 degradation and splicing inhibition. This correlation demonstrates the importance of achieving efficient U4 degradation to effectively block splicing and subsequently allow clear observation of the activities of the U4 mutants.

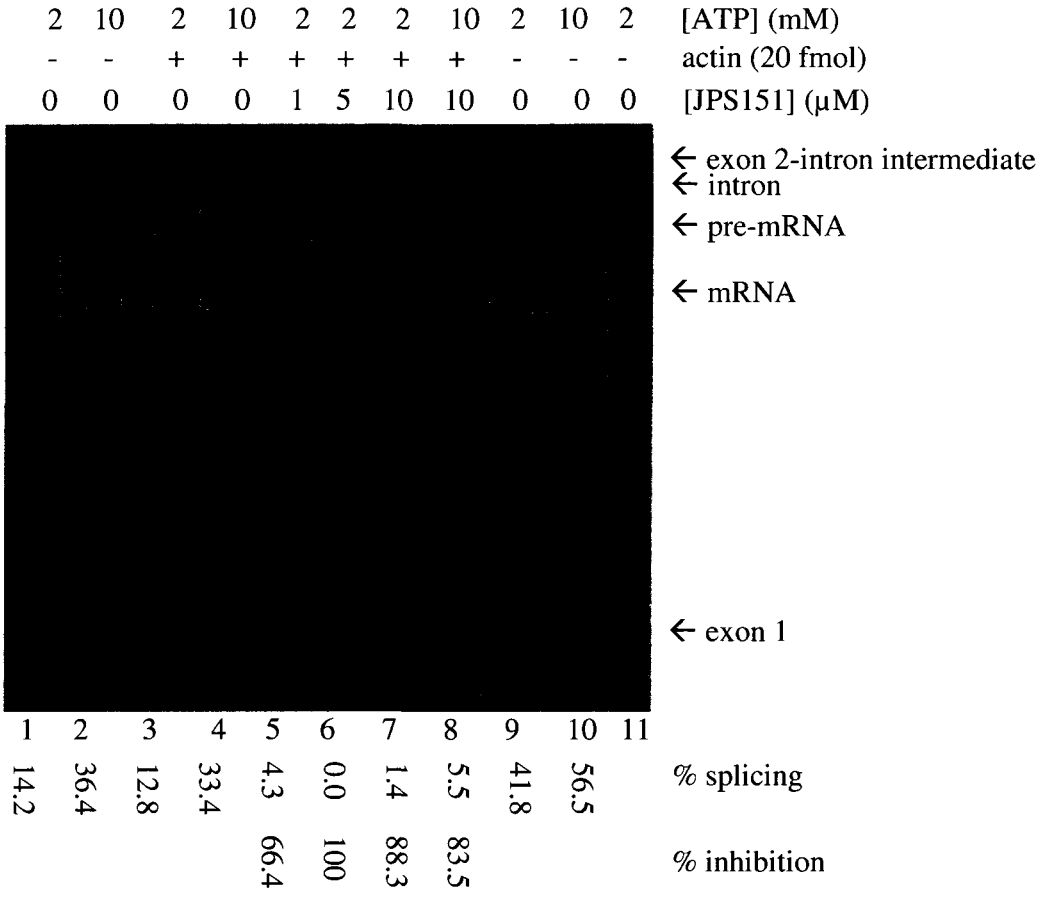

Figure 10. Degradation of U4 inhibits splicing. Splicing of ^{32}P-labeled actin pre-mRNA in extracts pre-treated with the indicated concentrations of oligo in the presence of 2 or 10mM ATP and in the presence or absence of 20 fmol unlabeled actin pre-mRNA. Lanes 9 and 10 are positive splicing controls and lane 11 is a negative splicing control. Splicing efficiency and splicing inhibition are indicated below the gel.

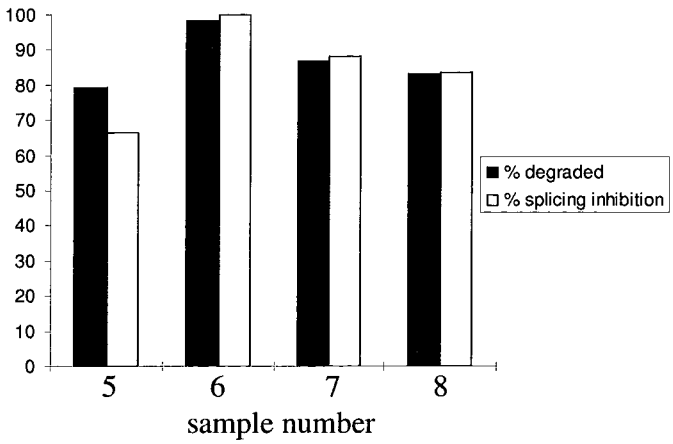

Figure 11. U4 degradation efficiency and splicing inhibition are closely correlated. Relationship between the fraction of U4 degraded and the degree of inhibition of splicing in samples 5-8 of Figures 9 and 10.

To identify the point in the splicing cycle at which U4 degradation caused a block, I examined spliceosome assembly in mock-depleted and U4-depleted splicing extract (Figure 12). While a time-course of spliceosome assembly in mock-depleted extract showed progression from pre-mRNA to the B complex and then the A complex, with appearance of mRNA at later time points (Figure 12a), examination of U4-depleted splicing extract showed that spliceosome assembly was blocked at the B complex (Figure 12b). Northern blot analysis confirmed the efficient degradation of U4 (Figure 12c). Only very low levels of the A complex were formed in the U4-depleted extract, and this was delayed compared to the mock-depleted extract. Consistent with denaturing gel analysis (Figure 10), no mature mRNA was formed in the U4-depleted extract (Figure 12b). These results suggest that U1 and U2 are able to associate with the pre-mRNA to form the B complex in the absence of an intact tri-snRNP, but further spliceosome assembly was blocked.

The observation that partial spliceosome assembly can still occur in U4-depleted extract strongly contradicts the holospliceosome model of spliceosome assembly. Contrary to the traditional accretion model of spliceosome assembly, which states that the pre-mRNA

interacts with individual snRNP particles in a stepwise manner (Figure 2), the holospliceosome model proposes that assembly occurs independently of the pre-mRNA and the pre-mRNA then interacts with a pre-formed penta-snRNP (Stevens *et al* .2002). Proposal of this model was prompted by the purification from yeast extract of a large particle containing the five snRNAs and 85% of all known splicing factors (Stevens *et al* .2002). When supplemented with micrococcal nuclease-treated extract, this particle was able to catalyze pre-mRNA splicing, and it did so as an intact particle that did not dissociate prior to binding the pre-mRNA (Stevens *et al* .2002). However, the results shown in Figure 12 suggest that, while interaction of the pre-mRNA with a preformed penta-snRNP may indeed occur in some cases, positioning of U1 and U2 within such a particle is not a prerequisite for interaction of these snRNPs with the pre-mRNA. This result is supported by a study by Behzadnia *et al.* (2006) in which it was found that U1 and U2 were still able to interact with pre-mRNA in human nuclear extract that had been affinity depleted of U4 and U6 and thus could not support formation of a holospliceosome. Furthermore, these pre-spliceosomes were shown to be active in splicing, indicating that they were functional intermediates in the spliceosome assembly pathway (Behzadnia *et al.* 2006). Together, these results suggest that active spliceosomes can be assembled on pre-mRNA in a step-wise manner and thus interaction with a pre-formed penta-snRNP, as proposed by the holospliceosome model, is not required.

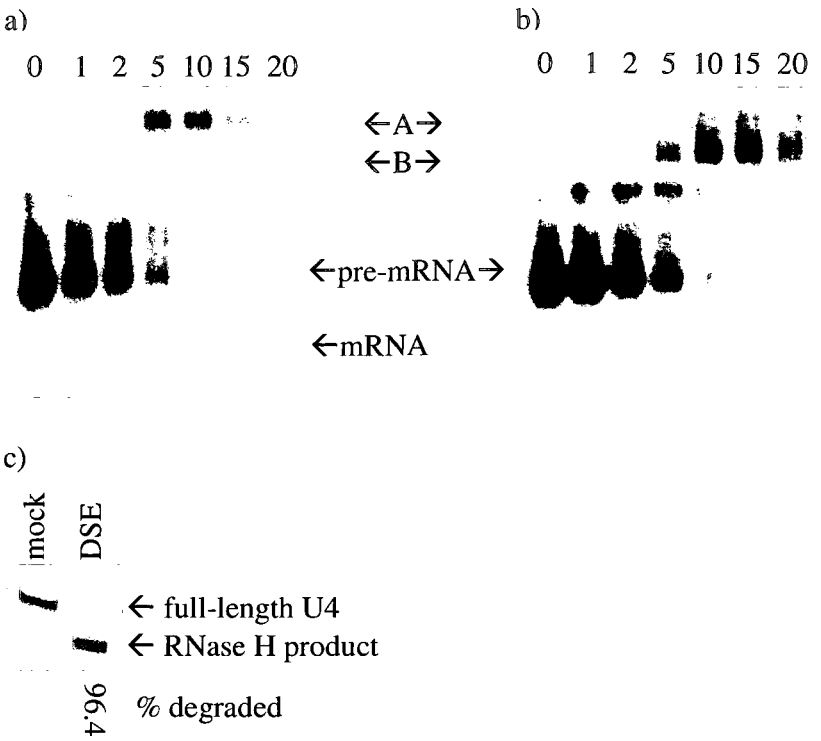

Figure 12. U4 degradation blocks spliceosome assembly at the B complex. Time-course of formation of assembly complexes on ^{32}P-labeled actin pre-mRNA in a) mock-depleted or b) U4-depleted splicing extract analyzed by non-denaturing gel electrophoresis. c) Northern blot showing U4 degradation in the U4-depleted splicing extract (DSE) used in part b).

A critical component of a splicing reaction is ATP, which serves as an energy source for the DEAD/DEXH-box proteins that catalyze RNA rearrangements within the spliceosome (Staley and Guthrie 1998). Previous examination of the effect of ATP concentration on splicing efficiency led to the current standard concentration of 2mM (Lin *et al.* 1985). However, Figure 11 shows that a significant increase in splicing efficiency was observed in the presence of a higher concentration of ATP (10mM). Titration of ATP showed that maximum splicing was obtained using 10mM ATP, and that splicing efficiency decreased with further increases in ATP concentration (Figure 13). I therefore used 10mM ATP in all subsequent experiments. The discrepancy between the optimal ATP concentration reported by Lin *et al.* (1985) and that observed here may be explained by differences in the

ATP requirements of the molecular machinery used to splice the two different pre-mRNA transcripts. It is also possible that differences in splicing extract preparation led to a higher concentration of ATP-consuming molecules, a lower concentration of ATP-regenerating molecules, or a lower concentration of endogenous ATP in the extract used here compared to that of Lin *et al.* (1985).

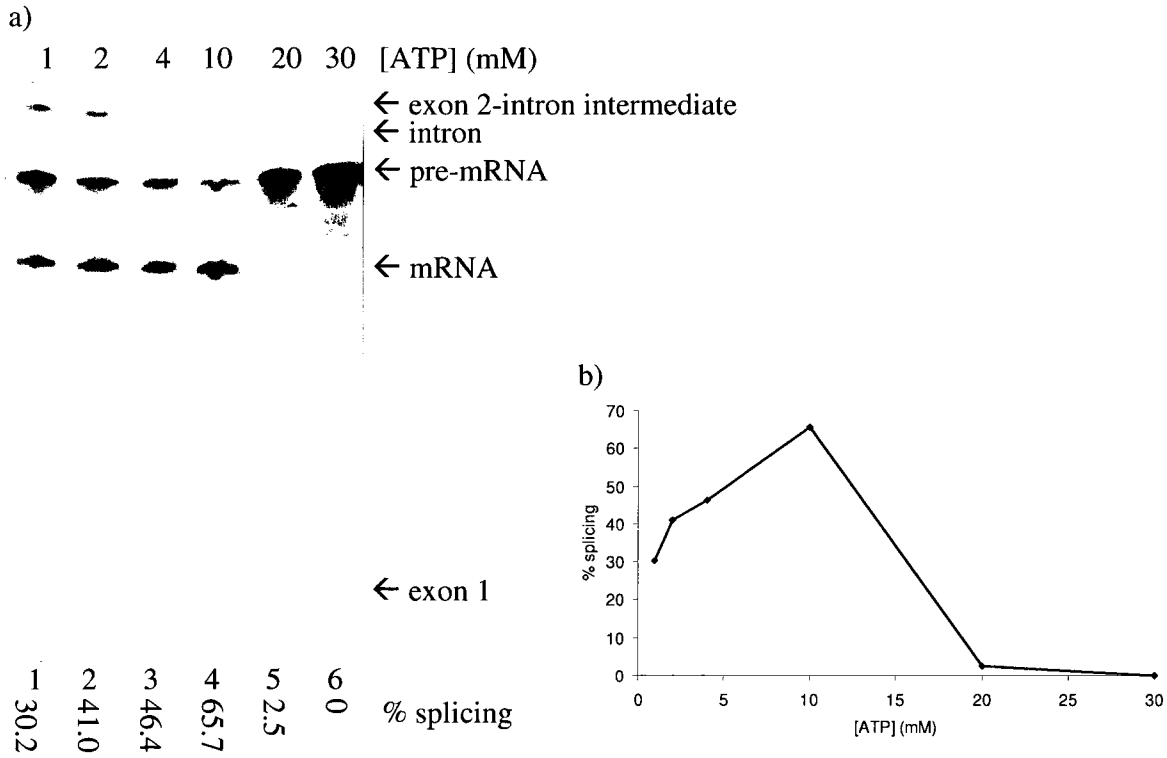

Figure 13. Maximum splicing efficiency is obtained with 10mM ATP. a) Splicing of actin pre-mRNA in reactions containing the indicated concentration of ATP. Splicing efficiency is indicated below the gel. b) Relationship between splicing efficiency and ATP concentration.

One final factor I examined during optimization of the U4 degradation reaction was the length of the targeting DNA oligonucleotide. Initial experiments used an oligonucleotide complementary to the stem II region of U4 (nucleotides 1-19) (JPS151). I examined a second oligonucleotide complementary to U4 nucleotides 1-30 (SDR553) for its ability to direct

RNase H degradation of U4. As SDR553 extends into the 5′ stem-loop, it produced a smaller degradation product than JPS151 (Figure 14). In addition, although the degradation efficiency of the two oligonucleotides was almost equal, the RNase H product of SDR553 was less stable than that of JPS151 (Figure 14). This was probably because SDR553 disrupts the 5′ stem-loop of U4, thereby making the remainder of the molecule more susceptible to degradation by endogenous nucleases in the extract. Conversely, U4 degradation directed by JPS151 leaves the 5′ stem-loop intact, thereby increasing resistance of the RNA fragment to exonuclease degradation. Given these results, I used SDR553 as the targeting oligonucleotide in all subsequent experiments. More complete degradation of U4 would result in better release of any bound proteins into the extract, making them available for assembly onto IVT U4 in reconstitution experiments. Furthermore, interference by the RNase H product in subsequent reconstitution experiments would be less likely using SDR553 than JPS151.

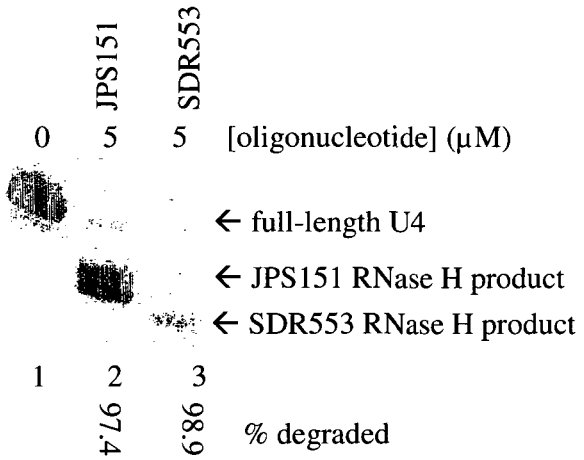

Figure 14. A longer targeting oligonucleotide results in more complete U4 degradation. Northern blot of U4 degradation in splicing extract incubated with the indicated concentration of oligonucleotide complementary to U4 nucleotides 1-19 (JPS151) or 1-30 (SDR553). U4 degradation efficiency is indicated below the gel.

CHAPTER 3

Identification of Optimal Conditions for Splicing Reconstitution in U4-Depleted Extract and Examination of Reconstitution by U4 3′ Truncation Mutants

A critical requirement for development of a U4 reconstitution assay is that addition of WT IVT U4 to the U4-depleted extract must result in restoration of splicing activity. I therefore examined a variety of reaction conditions to identify those allowing maximal reconstitution of splicing. Once these conditions had been established, I used this assay to examine the activities of three different U4 3′ truncation mutants. These experiments allowed identification of the minimum functional sequence of U4, and for the non-functional mutants, identification of where in the splicing cycle they caused a block. Together, these experiments further our understanding of the contributions of individual U4 snRNA functional domains to di-snRNP formation, spliceosome assembly, and splicing.

3.1 Materials and Methods

3.1.1 Stability and Activity of Reconstituted U4 snRNPs

Following the RNase H degradation reaction, I added the indicated concentration of IVT U4 and incubated the mixture at 23°C for 6 minutes to allow the RNA to interact with its specific proteins and participate in di- and tri-snRNP formation. To assess the stability of the IVT U4, I incubated the mixture at 23°C for a further 30 minutes, followed by addition of 200μL stop solution and analysis by Northern blot as described above. To assess the ability of IVT U4 to reconstitute splicing activity, I added 1μL ^{32}P-labeled actin pre-mRNA (4 fmol) to the extract following the 6 minute incubation, then incubated this reaction for a further 30

minutes at 23°C. Reactions were terminated by addition of 200μL stop solution and splicing activity was analyzed as described above.

3.1.2 Reconstitution of U4/U6 Base-Pairing

Following the RNase H degradation reaction, I added 300nM IVT U4 and incubated the mixture at 23°C for 6 minutes to allow interaction with U6 to occur. I then added 200μL stop solution and samples were phenol:chloroform extracted and ethanol precipitated as described above, except that the 5 minute incubation at 65°C following phenol:chloroform addition was omitted to avoid disruption of U6/U6 base-pairing. Precipitated RNA was resuspended in 10μL hybridization buffer (150mM NaCl, 50mM Tris-HCl (pH 7.4), 1mM EDTA) and incubated for 15 minutes at 23°C with 1μL ^{32}P-labeled oligonucleotide complementary to U4 (U4 14B) or U6 (SDR467). Samples were then mixed with 2μL 6x gel loading buffer (50% glycerol, trace bromophenol blue and xylene cyanol) and run 1 hour at 300V at 4°C on a pre-cooled 9% non-denaturing polyacrylamide gel. The gel was then exposed to a phosphor screen at -80°C.

To calculate annealing efficiency, autoradiograms were visualized and quantified using a Cyclone© phosphoimager and Optiquant© software (Packard Instruments). Annealing efficiency was calculated from the U6-probed samples by dividing the intensity of the U4/U6 band by the total intensity of both bands (U4/U6 and free U6).

3.1.3 Generation of U4 3' Truncation Mutants

I generated templates for transcription of the mutants by PCR from the U4-containing plasmid pT7U4. For all mutant templates, the same forward primer, containing the T7 promoter (indicated in bold), was used

SDR591

5' **AATTAATACGACTCACTATAGGG**ATCCTTATGCACGGGAAATA 3'

The reverse primers used were

SDR592 (for U4 1-68)

5' TTTCAACCAGCAAAAACA 3'

SDR593 (for U4 1-142)

5' CCCTACATAGTCTTGAAGTATTCA 3'

SDR595 (for U4 1-90)

5' GACGGTCTGGTTTATAATTAAATTTCA 3'

PCR products were purified on a 6% denaturing polyacrylamide gel prior to their use as templates in standard *in vitro* transcription reactions using the MEGAshortscript kit (Ambion 2008). Transcript was purified on a 6% denaturing polyacrylamide gel.

3.1.4 Reconstitution of Splicing, Spliceosome Assembly, and U4/U6 Base-Pairing by the U4 3' Truncation Mutants

I analyzed reconstitution of splicing and di-snRNP formation by the U4 3' truncation mutants as described previously for WT U4. Reconstitution of spliceosome assembly was analyzed as described previously, except that 300 nM WT or mutant IVT U4 was added to the U4-depleted splicing extract prior to the 30 minute incubation with ^{32}P-labeled actin pre-mRNA, and assembly complexes were separated by electrophoresis on a 4% non-denaturing polyacrylamide (80:1) gel in 1X TGM buffer (50mM tris base, 50mM glycine, 2mM $MgCl_2$) for 3 hours at 160V at 4°C.

3.2 Results and Discussion

3.2.1 Optimal Conditions for Splicing Reconstitution in U4-Depleted Extract

Previous experiments showed that targeting DNA oligonucleotide concentrations below 5μM did not efficiently degrade U4 or inhibit splicing (Figures 9 and 10). However, by using a new preparation of cold actin pre-mRNA to generate splicing conditions during the RNase H reaction, I saw efficient U4 degradation and splicing inhibition by as little as 0.5μM DNA oligonucleotide (Figure 15). Presumably, the better-quality actin resulted in increased splicing and thus more efficient release of free U4 snRNP, allowing a ten-fold reduction in the required concentration of targeting oligonucleotide. This oligonucleotide concentration is comparable to the 0.45 and 0.1-0.3μM concentrations reported for the degradation of yeast U2 and U6, respectively (McPheeters *et al.* 1989, Fabrizio *et al.* 1989). Underscoring the importance of performing U4 degradation under splicing conditions, Figure 15 also shows that, in the absence of splicing (lane 2), 5μM targeting oligonucleotide was required to achieve the level of degradation efficiency produced by 0.05μM targeting oligonucleotide in the presence of splicing (lane 5). Thus, performing U4 degradation under splicing conditions decreased the required oligonucleotide concentration by 100-fold.

Successful development of an *in vitro* splicing reconstitution assay requires that the method used for depletion of the target snRNA does not also cause depletion of the subsequently added IVT RNA. Although 5 and 0.5μM targeting oligonucleotide allowed efficient degradation of endogenous U4, they also result in nearly complete degradation of the IVT U4 (Figure 15, lanes 3, 4, 8, and 9). While degradation of IVT U4 is decreased in splicing extract containing 0.05μM targeting oligonucleotide, this oligonucleotide

concentration is not sufficient for efficient degradation of endogenous U4 (Figure 15, lanes 5 and 9).

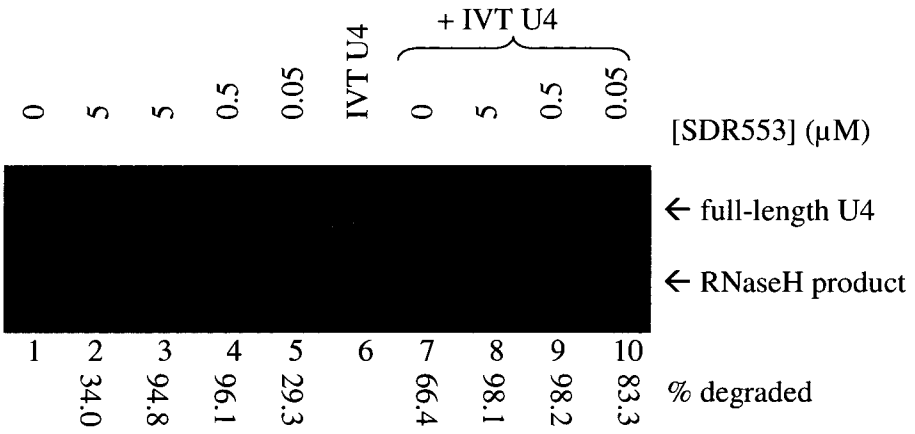

Figure 15. Lower oligonucleotide concentrations improve IVT U4 stability. Northern blot showing degradation of endogenousU4 (lanes 1-5) and stability of 50 fmol IVT U4 in the presence of the indicated concentrations SDR553. The RNase H reaction in lane 2 was performed under non-splicing conditions. Lane 6 contains only 50 fmol IVT U4. The fraction of endogenous or IVT U4 degraded in each reaction is indicated below the gel.

Based on the results shown in Figure 15, I examined a range of targeting oligonucleotide concentrations between 0.05 and 0.5μM in an attempt to identify a concentration that allowed efficient degradation of endogenous U4 but not IVT U4 (Figure 16). However, oligonucleotide concentrations below 0.5μM resulted in a decreased U4 degradation efficiency and were therefore less effective at blocking splicing (Figure 16, lanes 2 and 3).

Given that previous studies achieved RNase H degradation of snRNAs in yeast extract without additional enzyme (McPheeters *et al.* 1989, Fabrizio *et al.* 1989), I re-examined U4 degradation in the absence of exogenous RNase H (Figure 16, lane 5). Contrary to initial results (Figure 5), I found the efficiency of U4 degradation and splicing inhibition with 0.5μM oligonucleotide to be independent of exogenous RNase H (Figure 16, lanes 4

and 5). Again, this change may have been due to the use of better-quality actin, which would have increased accessibility of the 5′ end of U4 and thereby decreased the RNase H concentration required for interaction with, and subsequent degradation of, this region of U4. Importantly, IVT U4 was more stable in extract depleted of U4 without additional RNase H (Figure 16a, lanes 10 and 11). Therefore, subsequent reactions contained 0.5μM oligonucleotide and no exogenous RNase H.

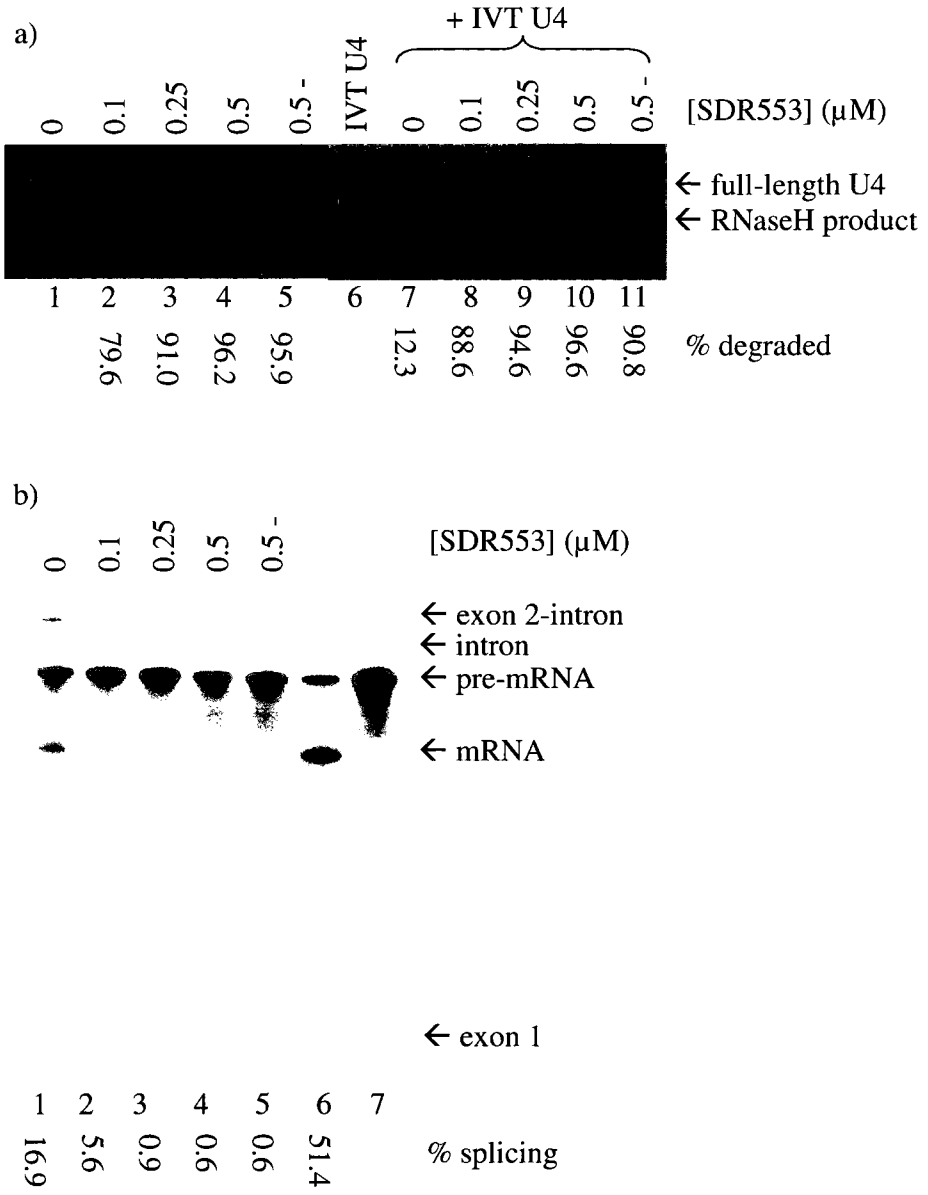

Figure 16. U4 degradation and splicing inhibition is independent of exogenous RNase H. a) Degradation of endogenous U4 and stability of 50 fmol IVT U4 in the presence of the indicated concentrations of SDR553 and b) the effect on splicing. Lanes 6 and 7 of b) are positive and negative splicing controls, respectively. Lane 6 of a) contains only 50 fmol IVT U4. The negative sign (-) indicates no added RNase H. The efficiency of U4 degradation (a) or splicing (b) is indicated below the gels.

As suggested by the improved stability of IVT U4, these U4 depletion conditions (0.5μM oligonucleotide and no exogenous RNase H) allowed successful reconstitution of splicing in U4-depleted extract following addition of IVT U4 (Figure 17a). The efficiency of splicing in mock-depleted extract, 58.9%, was decreased to 5.4% upon depletion of endogenous U4, and restored to 18.5% by addition of IVT U4 (Figure 17a). Titration of IVT U4 showed that maximum reconstitution was achieved by the addition of 300nM IVT U4 (Figure 17b). The decrease in reconstitution efficiency by IVT U4 concentrations above 300nM may be due to increased competition for U4-specific proteins, effectively diluting the proteins available, such that fewer U4 RNA molecules receive the full protein complement needed to be functional.

The concentration of IVT U4 found here to be required for maximum reconstitution was substantially higher than the values reported for maximum reconstitution of yeast U2 (40nM) and U6 (10nM), despite the fact that the latter two snRNAs are found at a higher endogenous concentration in splicing extract (McPheeters *et al.* 1989, Fabrizio *et al.* 1989). Specifically, the concentration of IVT U4 required here for maximum reconstitution was approximately 150-fold higher than the concentration of endogenous U4 present in the mock-depleted splicing extract (determined by Northern blot analysis comparing to IVT U4 standards, data not shown), while the concentrations of yeast U2 and U6 required for maximum reconstitution were approximately eight- and two-fold the endogenous levels, respectively (McPheeters *et al.* 1989, Fabrizio *et al.* 1989).

There are several possible explanations for the substantially higher concentration of *in vitro* transcript required for reconstitution of U4 compared to U2 and U6. One possibility is that a higher proportion of IVT U4 was degraded by nucleases upon addition to extract.

Since a higher concentration of targeting oligonucleotide was used to deplete U4 than U2 and U6 (0.5 μM compared to 0.1-0.3 μM and 0.45 μM, respectively (McPheeters *et al.* 1989, Fabrizio *et al.* 1989)), a higher concentration of the oligonucleotide may have remained in the extract at the time of IVT U4 addition, causing a greater fraction of the IVT U4 to be degraded by residual RNase H activity. Furthermore, differences in extract preparations may have led to higher levels of endogenous DNase activity in the extracts of McPheeters *et al.* (1989) and Fabrizio *et al.* (1989) compared to the extracts I used, contributing to decreased degradation of the DNA oligonucleotide and therefore increased degradation of IVT U4.

It is also possible that, due to sequence and conformational differences between the three snRNAs, IVT U4 may be more susceptible to degradation by nucleases in the extract than U2 or U6. Since the snRNAs are stabilized by interaction with their specific proteins, it may be that U2 and U6 form such interactions more readily than U4. Another possibility is that only a fraction of the IVT U4 was in an active conformation, and that this fraction was lower than that for U2 or U6. One possible source of such inactivity is misincorporation by T7 RNA polymerase during transcription. Although the error rate of this enzyme is low (Huang *et al.* 2000), it has been shown to have increased susceptibility to slippage when transcribing regions of a template with extended stretches of adenosine or thymine (Reyes and Abelson 1988). As the U4 template contains a number of regions composed entirely of adenosine and thymine, up to 15 nucleotides in length, such errors may have contributed to the non-functionality of a significant portion of the IVT U4. Finally, inactivation of a portion of U4 may have been caused by incorrect folding of the *in vitro* transcript. Indeed, the separation of IVT U4 by non-denaturing gel electrophoresis suggested that the majority of this molecule may in fact adopt a conformation different from that of endogenous U4 (Figure

19, lane 4). As IVT U4 runs as a single band when analyzed on a denaturing gel (Figures 15 and 16, lane 6), this observation supports the hypothesis that the two IVT U4 bands seen under non-denaturing conditions do indeed reflect a conformational difference and not a difference in transcript length. It would be expected that increasing the fraction of correctly folded U4, such as through glycerol gradient purification, would decrease the concentration of U4 necessary for maximum splicing reconstitution.

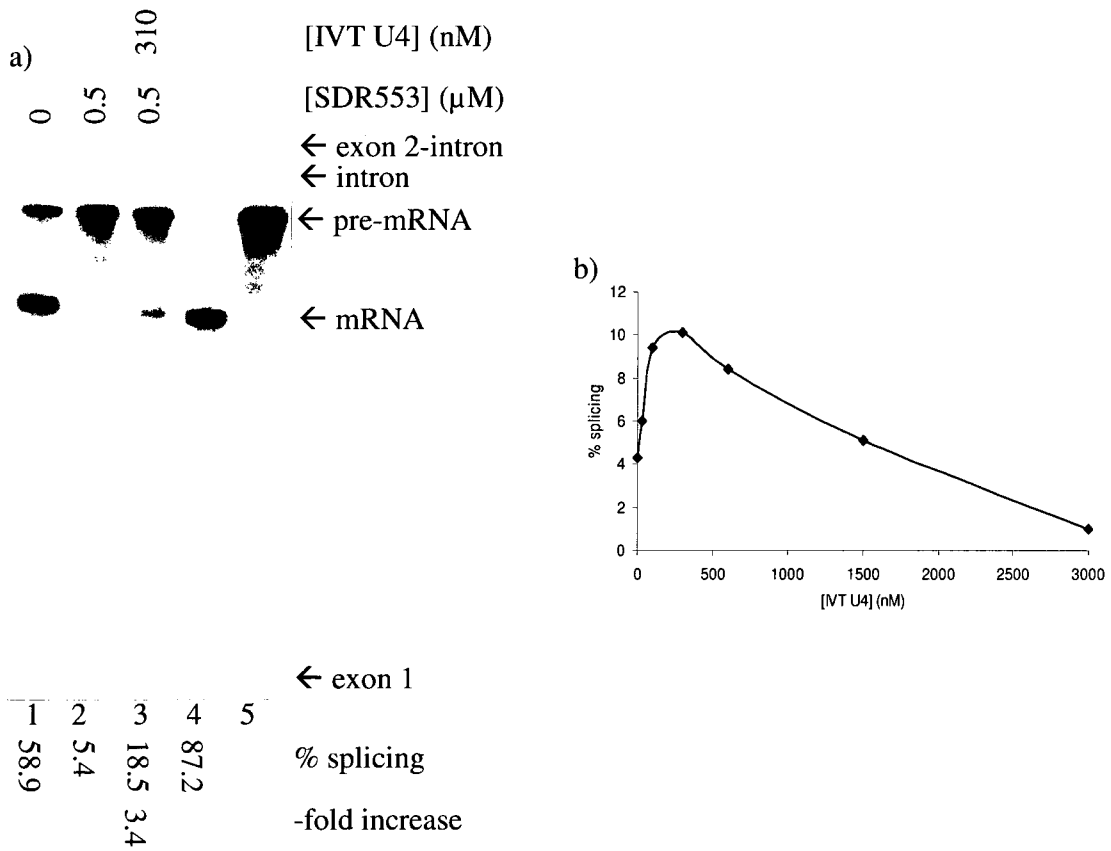

Figure 17. Splicing in U4-depleted extract is reconstituted by IVT U4. a) Splicing in mock depleted (lane 1) or U4-depleted (lanes 2 and 3) splicing extract in the absence (lanes 1 and 2) or presence (lane 3) of 310 nM IVT U4. Lanes 4 and 5 are positive and negative splicing controls, respectively. Splicing efficiency and fold increase in splicing upon reconstitution are shown below the gel. b) Relationship between the concentration of IVT U4 and the level of splicing reconstituted.

As efficiency of splicing reconstitution is a measure of the fold increase in splicing in U4-depleted splicing extract upon addition of IVT U4, I examined a number of oligonucleotide concentrations around 0.5μM for any concentrations that amplified the difference between splicing efficiency before and after IVT U4 addition. While a lower oligonucleotide concentration resulted in a substantially smaller increase in splicing upon reconstitution (Figure 18), slightly higher oligonucleotide concentrations improved reconstitution efficiency, with 0.8μM oligonucleotide giving the largest increase at 35.6-fold above the U4-depleted extract (Figure 18). Therefore, subsequent U4 degradation reactions were performed using 0.8μM targeting oligonucleotide.

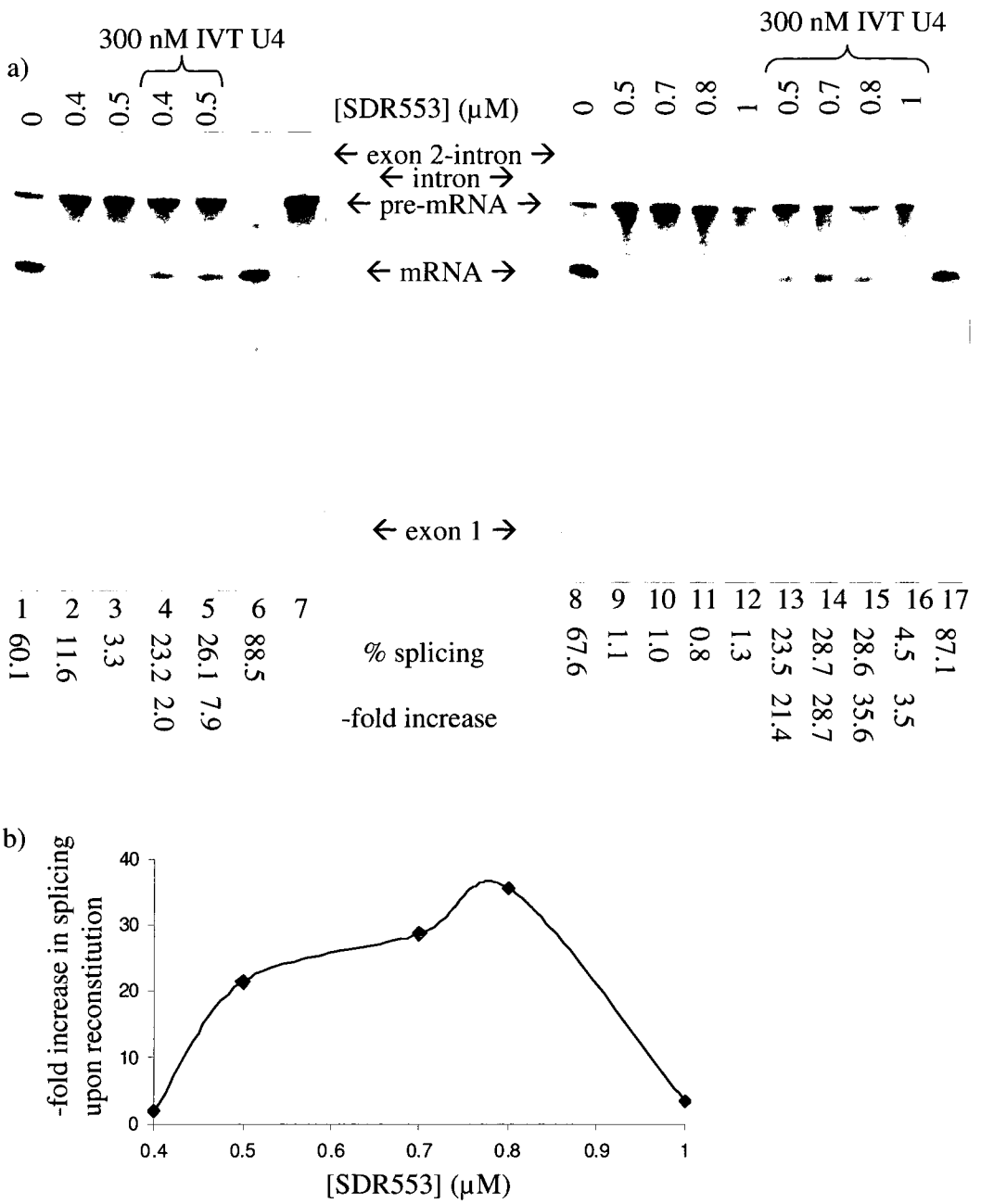

Figure 18. 0.8μM oligonucleotide allows maximal reconstitution. a) Inhibition of splicing by incubation of extract with 0.4 to 1 μM SDR553 and reconstitution of splicing by addition of 300 nM IVT U4. Lanes 6 and 17 are positive splicing controls and lane 7 is a negative splicing control. Splicing efficiency and fold increase in splicing upon reconstitution are shown below the gel. b) Relationship between oligonucleotide concentration and the increase in splicing in U4-depleted extract upon addition of 300 nM IVT U4.

As U4 forms an extensive base-pairing interaction with U6, I examined its disruption by U4 depletion and reconstitution by addition of IVT U4 by non-denaturing gel electrophoresis. Figure 19 shows that U4 degradation effectively eliminated detection of the di-snRNA species, which was reconstituted by incubation with IVT U4. As an extended incubation period did not improve the efficiency of U4/U6 reconstitution (Figure 19, lanes 5 and 10), a six minute incubation was used in subsequent experiments.

While reconstituted samples probed for U6 showed a clear re-formation of the di-snRNA, reconstituted samples probed for U4 showed only a very faint band at the position of U4/U6 (Figure 19, lanes 4 and 5). Although the 3′ region of U4 bound by the probe should be equally accessible in the free U4 and U4/U6 species, if free U4 was preferentially bound, this may have led to a shortage of probe available to bind U4 in the di-snRNA, resulting in the observed lack of U4/U6 signal in these samples. Given the clear disruption of U4/U6 in U4-depleted extract and reconstitution of this species by addition of IVT U4 when the base-pairing status of U6 is observed (Figure 19, lanes 8-10), subsequent experiments examining reconstitution of U4/U6 were performed using a U6 probe.

As discussed above, probing for U4 revealed that a substantial portion of the IVT U4 added to the U4-depleted splicing extract was in an alternate conformation which migrated more slowly than the endogenous U4 (Figure 19, lanes 4 and 5). If such a conformation is nonfunctional, then separation of this species from the correctly folded U4 prior to reconstitution would substantially reduce the U4 concentration required for maximum splicing reconstitution.

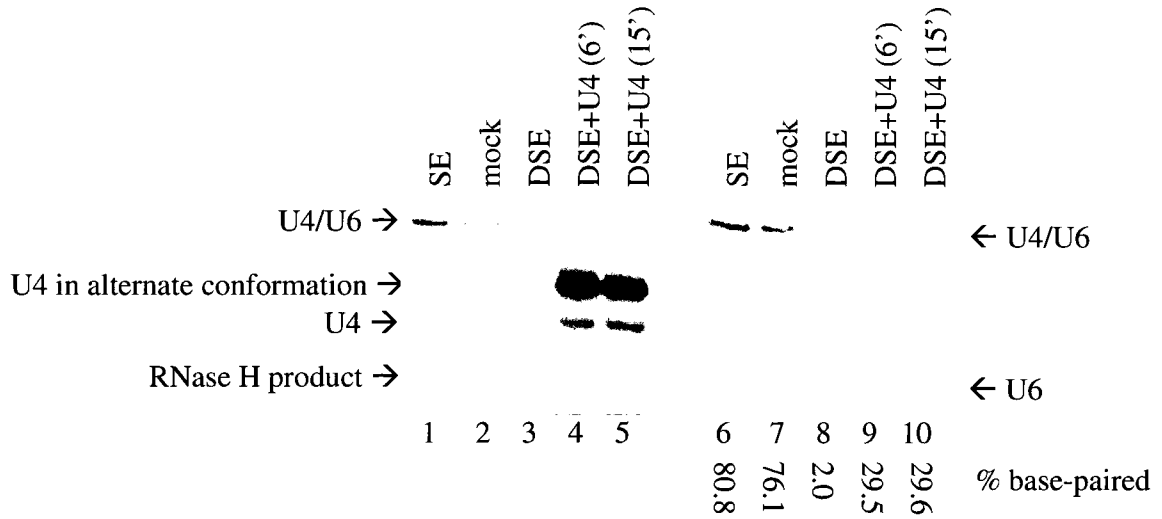

Figure 19. U4/U6 base-pairing in U4-depleted splicing extract is reconstituted by IVT U4. Non-denaturing gel showing the base-pairing status of U4 (lanes 1-5) and U6 (lanes 6-10) in untreated splicing extract (SE), mock depleted splicing extract, or U4-depleted splicing extract (DSE) in the absence or presence of 300 nM IVT U4 and incubated for 6 or 15 minutes. The percent of U6 base-paired to U4 is shown below the gel.

3.2.2 Analysis of U4 3′ Functional Domains

3.2.2.1 Phylogenetic and Mutational Analysis of the 3′ Portion of U4 snRNA

As functionally significant regions of biomolecules are under greater selective pressure and therefore display stronger evolutionary conservation, phylogenetic analysis is a valuable means of identifying functionally important domains of these molecules. Such analysis of U4 snRNA reveals considerable variation of conservation across the molecule. While the 3′ half of U4 is generally less well conserved than the 5′ portion (Guthrie and Patterson 1988, Myslinski and Branlant 1991), certain regions within the 3′ portion do display a significant level of conservation.

One highly conserved region in the 3′ portion of U4 is the poly-uridine tract (Guthrie and Patterson 1988, Myslinski and Branlant 1991) that serves as a binding site for the Sm

proteins (Figure 20), which are important for nuclear localization of the snRNA (Fischer *et al.* 1993). Accordingly, deletion of the Sm-binding site blocks splicing *in vivo*, since the snRNA is not localized to the nucleus (Vankan *et al.* 1990). Similarly, point mutations in the Sm-binding site of yeast U4 are lethal or conditionally lethal *in vivo* (Hu *et al.* 1995). However, the Sm-binding site was not found to be required for spliceosome assembly or splicing *in vitro* in human nuclear extract (Wersig and Bindereif 1990, 1992).

The 3′ stem-loop is a highly variable domain of U4, both in size and sequence (Guthrie and Patterson 1988, Myslinski and Branlant 1991) (Figure 20). Consistent with this extreme phylogenetic variability, Vankan *et al.* (1990) demonstrated this region to be dispensable for splicing in *Xenopus* oocytes. Similarly, Wersig and Bindereif (1990, 1992) showed that this region of human U4 is not essential for spliceosome assembly or splicing in human nuclear extract, although its deletion does cause a reduction in splicing activity. Conversely, using an *in vivo* assay, Bordonne *et al.* (1990) found the 3′ stem-loop to be an essential element of U4 in yeast; substitution with the comparable region of *Trypanosoma brucei* U4 resulted in significant inhibition of di-snRNP assembly and was lethal. Similarly, *in vivo* experiments by Hu *et al.* (1995) found that deletion of nucleotides 131-133 within the 3′ stem-loop of yeast U4 resulted in conditional lethality. The incongruence of these results may reflect differences in the splicing mechanisms of the organisms being studied, such as the mechanism of di-snRNP formation; differences between the *in vivo* and *in vitro* assays used; or simply differences in the snRNA sequence requirements for splicing of the pre-mRNAs being studied (Vankan *et al.* 1990).

A second highly conserved sequence in the 3′ portion of U4 is the 5′ region of the single-stranded central domain (Vankan *et al.* 1990, Guthrie and Patterson 1988) (Figure 20).

Consistent with its conservation, deletion of this sequence strongly inhibits splicing in human nuclear extract and *Xenopus* oocytes, while deletions in the remaining portion of the central domain have a substantially decreased effect on splicing (Wersig and Bindereif 1992, Vankan *et al.* 1992). Interestingly, deletion of the entire central domain of yeast U4 resulted in only a mild conditional growth defect (Hu *et al.* 1995), again suggesting differences in the U4 sequence requirements of these organisms.

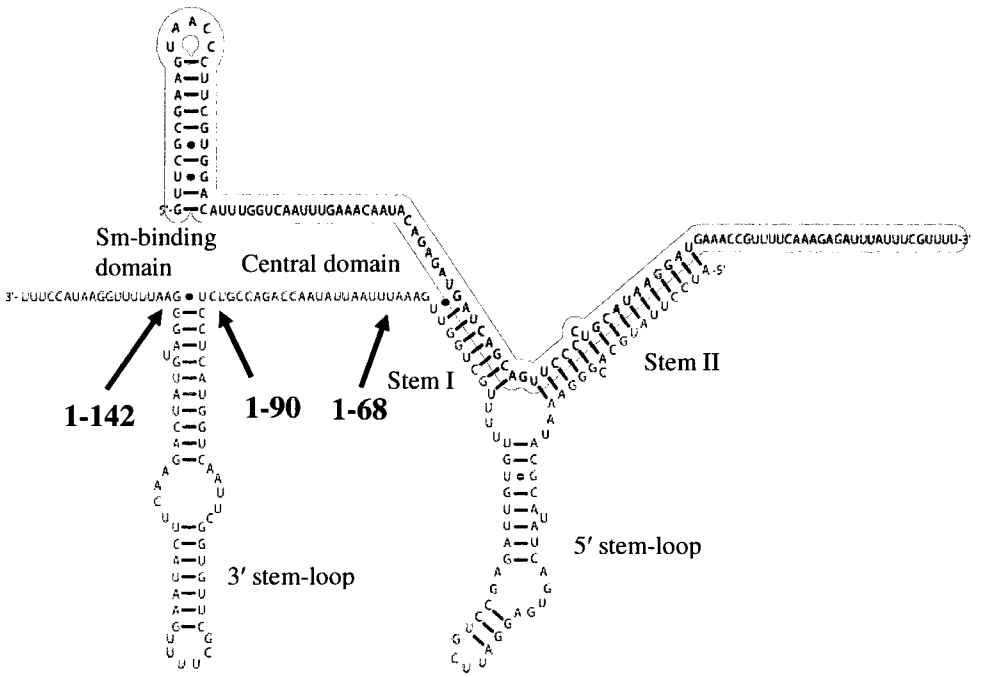

Figure 20. U4 3′ truncation mutants. Secondary structure of U4 (yellow) in the di-snRNA with positions used to generate U4 3′ truncation mutants indicated by arrows.

3.2.2.2 Reconstitution of Splicing, Spliceosome Assembly, and U4/U6 Base-Pairing by U4 3′ Truncation Mutants

Given the above analyses of U4 3′ domains required for splicing, as well as the observation that the 5′ stem-loop and stems I and II are all required for efficient spliceosome assembly and splicing (Wersig and Bindereif 1990, 1992; Vankan *et al.* 1990), I began my

search for the minimum U4 sequence able to support splicing by examining a U4 mutant containing only nucleotides 1-68. This mutant lacked the Sm-binding site, the 3′ stem-loop, and most of the central domain (Figure 20), though it did contain the 5′ portion of the central domain identified by Wersig and Bindereif (1992) and Vankan *et al.* (1992) as being important for splicing activity. I generated the template for transcription of this mutant by PCR, as described in the methods, and tested its ability to participate in splicing.

To examine the effect of removing the 3′ end of U4, I added the truncated U4 transcript to extract depleted of endogenous U4 and assessed its ability to restore splicing of pre-mRNA. Unexpectedly, addition of U4 1-68 to the U4-depleted extract did not result in any reconstitution of splicing activity (Figure 21, lane 5). To confirm that the extract was functional, I also examined addition of WT U4, which restored splicing to 15.3% from 1.2% in the U4-depleted extract (Figure 21, lane 3). In mock depleted extract, 57.2% of the pre-mRNA was spliced. These results establish that the extract was active, that splicing was successfully blocked by depletion of endogenous U4 and reconstituted by addition of WT IVT U4, and therefore that the failure of U4 1-68 to restore splicing, while a negative result, was nevertheless credible.

Lack of splicing reconstitution by U4 1-68 may have been due to the absence of the 3′ portion of the central domain. While not as important for splicing as the 5′ region of the central domain, deletion of this sequence still had an appreciable effect on splicing (Wersig and Bindereif 1992). Therefore, I synthesized a longer 3′ truncation mutant containing the entire central domain (U4 1-90, Figure 20) and examined its activity using the reconstitution assay. However, Figure 21 (lane 6) shows that this mutant also was unable to reconstitute splicing.

The final U4 3′ truncation mutant I examined, U4 1-142, was truncated just 3′ of the 3′ stem-loop and thus lacked the Sm protein binding site (Figure 20). Consistent with reconstitution studies in human nuclear extract (Wersig and Bindereif 1992), I found this region of yeast U4 to be dispensable for splicing *in vitro,* as it yielded an approximately 10-fold increase in splicing over the U4-depleted extract (Figure 21, lane 4).

Together, these results suggest that the function of the U4 Sm proteins is largely limited to proper cellular localization of the snRNP *in vivo,* with no further roles that are required for splicing *in vitro.* In contrast, examination of the U1 snRNP has shown that the Sm proteins are essential for snRNP assembly (Hamm *et al.* 1990), and a recent crystal structure of the U1 snRNP has shown that this is due to their role in stabilizing RNA structures required for further protein assembly (Krummel *et al.* 2009). Thus, the results of this study highlight important differences between the mechanisms of protein assembly during the biogenesis of different snRNAs.

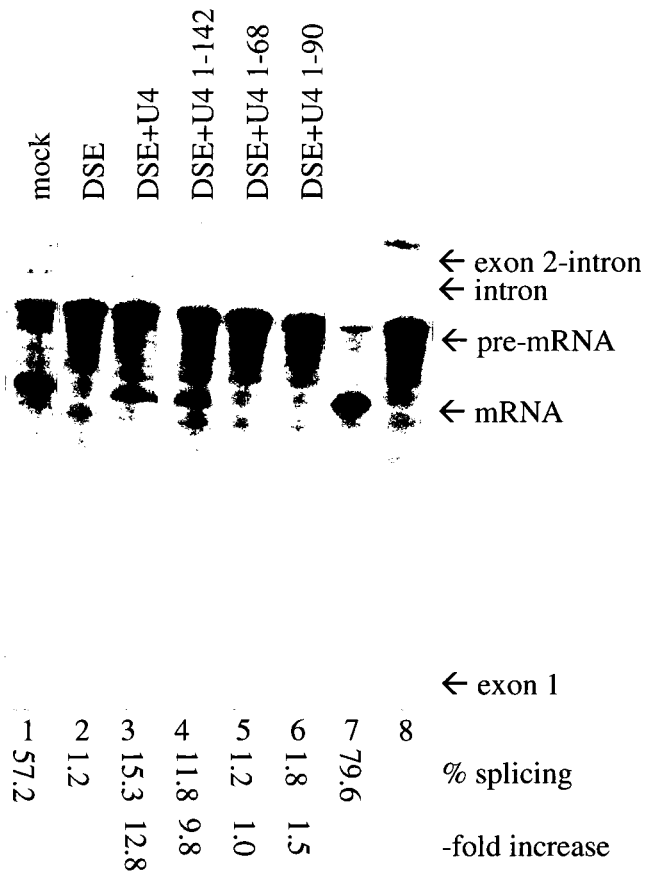

Figure 21. Splicing is reconstituted by U4 1-142, but not U4 1-68 or U4 1-90. Splicing in mock depleted (lane 1) or U4-depleted (lane 2-6) splicing extract in the absence (lane 2) or presence of 300nM IVT WT (lane 3) or 3′ truncated (lanes4-6) U4. Lanes 7 and 8 are positive and negative splicing controls, respectively. Splicing efficiency and fold increase in splicing upon reconstitution are shown below the gel.

While the lack of splicing reconstitution by U4 1-68 and 1-90 may have been due to exclusion of a functionally essential region of the molecule, it may also have resulted from decreased stability of these mutants in splicing extract. To investigate this possibility, I used Northern blot analysis to examine the stability of WT and mutant IVT U4 snRNA in U4-depleted splicing extract. Figure 22 shows that approximately half of the WT IVT U4 added to U4-depleted splicing extract remained at the end of the reconstitution assay (lanes 1 and

5). This is similar to the stability of IVT U2 in U2-depleted yeast extract, where approximately 35% of the input RNA was stable during the reconstitution assay (McPheeters *et al.* 1989). While previous studies report the stabilities of WT and mutant snRNAs during the reconstitution assay to be roughly similar (McPheeters *et al.* 1989, Fabrizio *et al.* 1989, Wersig and Bindereif 1992), I observed decreased stability of the mutants relative to WT U4 (Figure 22). However, lack of reconstitution by U4 1-68 and 1-90 cannot be entirely attributed to transcript degradation, since U4 1-90, which was more stable than U4 1-142, did not reconstitute splicing, while U4 1-142 did (Figures 21 and 22). This suggests that the inability of U4 1-90 to reconstitute splicing was not due to a lack of stability; rather, the results suggest that this mutant lacks some functionally essential component of U4. Furthermore, while U4 1-68 was the least stable of the mutants (Figure 22), the inactivity of U4 1-90 implies that this even-shorter mutant would be unable to reconstitute splicing even if it was completely stable during the reconstitution assay.

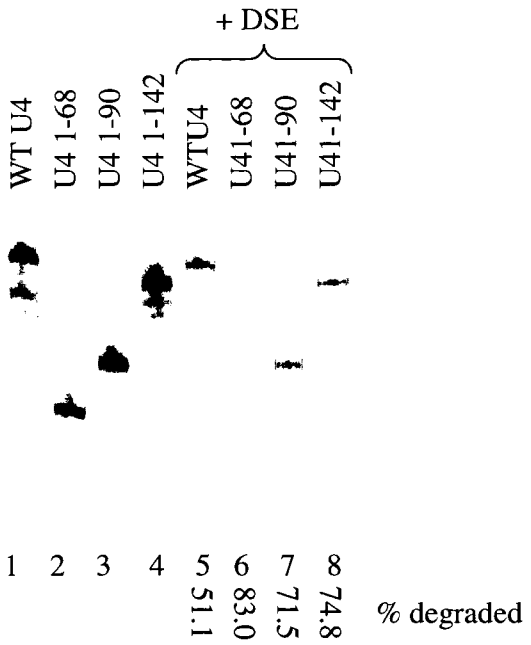

Figure 22. Stability of U4 mutants in U4-depleted splicing extract is variable. Northern blot showing stabilities of WT and mutant IVT U4 in the absence (lanes 1-4) or presence (lanes 5-8) of U4-depleted splicing extract (DSE). U4 degradation efficiency is indicated below the gel.

To further explore the lack of splicing reconstitution by U4 1-68 and 1-90 in U4-depleted extract, I investigated the ability of these mutants to reconstitute spliceosome assembly (Figure 23). Figure 12 shows that degradation of U4 blocks spliceosome assembly at complex B and prevents accumulation of mature mRNA (Figure 23, lane 4). Addition of WT U4 or U4 1-142 restored formation of complex A and mature mRNA, while addition of U4 1-68 or 1-90 did not (Figure 23, lanes 5-8). These results suggest that the lack of splicing reconstitution by U4 1-68 and 1-90 is due to an inability of these mutants to participate in spliceosome assembly.

Furthermore, this experiment suggests that regions of U4 beyond the U6-activating sequence predicted by the Dunn-Rader model (U4 stem II, see Figure 4) are required for stable binding of U6 to the pre-mRNA. If the U4 3′ truncation mutants containing stem II had

been sufficient for U6/pre-mRNA interaction, even if further spliceosome assembly was blocked, accumulation of a band between complexes H and B, corresponding to a U4/U6/pre-mRNA complex, would have been expected. The absence of such a band (Figure 23) suggests that either such a complex did not form, or if it did form, the absence of the deleted sequences and any associated protein factors caused the complex to be too unstable to be detected using this technique. Hence, the results of this experiment do not support the most direct prediction of the Dunn-Rader model of free U6, namely that the stem II region of U4 should be sufficient to open up U6 for interaction with pre-mRNA. This suggests that, if the Dunn-Rader model is correct, either the 3′ portions of U4 or their associated proteins are also important for U6 activation.

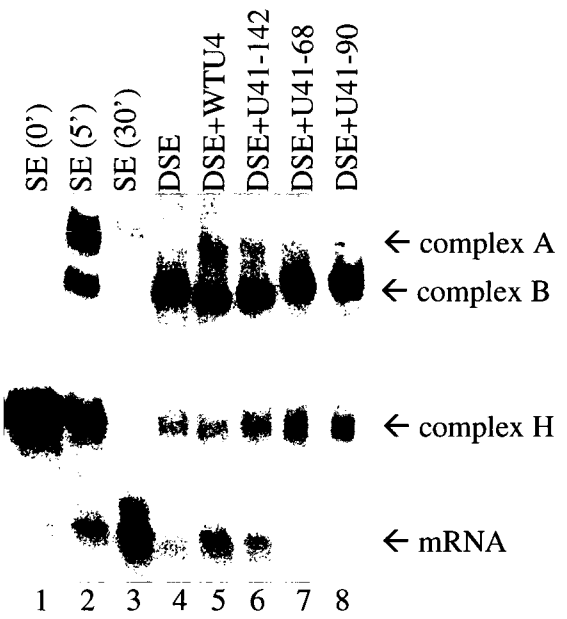

Figure 23. Formation of complex A is reconstituted by U4 1-142, but not by U4 1-68 or U4 1-90. Non-denaturing gel showing the assembly of spliceosomal complexes A and B on ^{32}P-labeled actin pre-mRNA incubated in splicing extract for the indicated times (lanes 1-3) or in U4-depleted splicing extract for 30 minutes (lanes 4-8) in the absence (lane 4) or presence (lanes5-8) of 300 nM WT or mutant IVT U4.

The lack of reconstitution of complex A formation by U4 1-68 and 1-90 could have been due to an inability of the mutants to interact with U6, an inability of the di-snRNP formed by U6 and the U4 mutants to interact with U5 to form a functional tri-snRNP, or an inability of the U4 mutant-containing tri-snRNP to interact with the pre-mRNA. To distinguish among these possibilities, I examined interaction between the U4 mutants and U6. Figure 24 shows that, while WT U4 and U4 1-142 were able to reconstitute formation of the di-snRNP in U4-depleted extract, U4 1-68 and 1-90 were not. Hence, the inability of U4 1-68 and 1-90 to reconstitute splicing stems from an inability to interact with U6. Furthermore, the ability of U4 1-142, but not U4 1-90, to interact with U6 implies that the 3′ stem-loop plays an essential role in formation of the di-snRNP. Given this result, it was impossible to draw any conclusions regarding the validity of the Dunn-Rader structural model of free U6 from these reconstitution experiments; while it is possible that only U4 stem II is required to expose the pre-mRNA-binding sequence of U6, a larger region of U4 is apparently necessary to establish U4/U6 interaction in the first place, thereby preventing separation of these two functions.

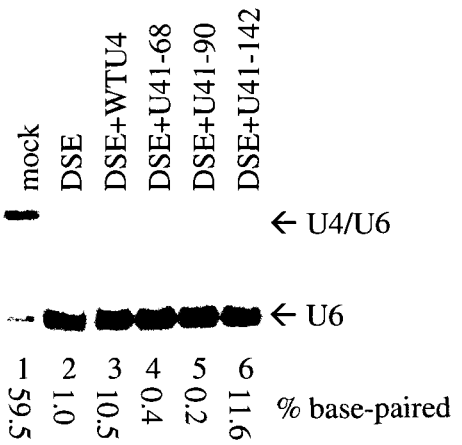

Figure 24. U4/U6 base-pairing is reconstituted by U4 1-142, but not U4 1-68 or U4 1-90. Non-denaturing gel showing the base-pairing status of U6 in mock depleted splicing extract (lane 1) or U4-depleted splicing extract (lanes 2-6) in the absence (lanes 1 and 2) or presence (lanes 3-6) of 300 nM WT or mutant IVT U4. The percent of U6 base-paired to U4 is shown below the gel.

The inability of U4 truncation mutants lacking the 3′ stem-loop to form the U4/U6 di-snRNP prevented use of the reconstitution assay to investigate whether this region may also function at later steps of spliceosome assembly or splicing. To investigate a possible role for this domain beyond di-snRNP formation, I performed RNase H degradation of the central domain of U4 under non-splicing conditions (unlabeled actin pre-mRNA was omitted), such that the U4/U6 interaction was maintained. This reaction produced a di-snRNP particle containing U6 base-paired to a U4 fragment composed of stems I and II and the intervening 5′ stem-loop (Figure 20). Truncation of U4 was confirmed by Northern blot analysis (Figure 25a, lane 3) and association with U6 was confirmed by non-denaturing gel electrophoresis (data not shown). Addition of ^{32}P-labeled actin pre-mRNA showed that the di-snRNP containing this 5′ portion of U4 was able to participate in splicing (Figure 25b, lane 3). However, if the U4 degradation reaction was performed under conditions of active splicing such that the U4/U6 interaction was disrupted (confirmed by non-denaturing gel

electrophoresis, data not shown), the same U4 fragment was produced (Figure 25a, lane 2), but subsequent splicing of ^{32}P-labeled actin pre-mRNA was blocked (Figure 25b, lane 2). Hence, extract containing the truncated form of U4 was only able to support splicing if U4 remained bound to U6; if the truncated U4 was dissociated from U6 prior to addition of ^{32}P-labeled actin pre-mRNA, splicing was blocked. It is interesting to note that splicing efficiency in extract containing the 5′ portion of U4 still bound to U6 was approximately three-fold lower than that in mock-depleted extract containing WT U4 (Figure 25b, lanes 1 and 3). Given that disruption of the interaction between U6 and the 5′ fragment of U4 blocked subsequent splicing (Figure 25b, lane 2), these results suggest that the observed difference in splicing efficiency between lanes 1 and 3 of Figure 25b may reflect the ability of the truncated U4-containing di-snRNP to support only a single round of splicing, while WT U4 was able to reanneal to U6 to allow multiple rounds of splicing. Taken together, these results indicate that, while the portion of U4 3′ of stem I is required for interaction with U6, it does not contribute to later steps of spliceosome assembly or splicing catalysis. This is consistent with previous experiments presented here that suggest that the 3′ stem-loop plays a critical role in di-snRNP formation.

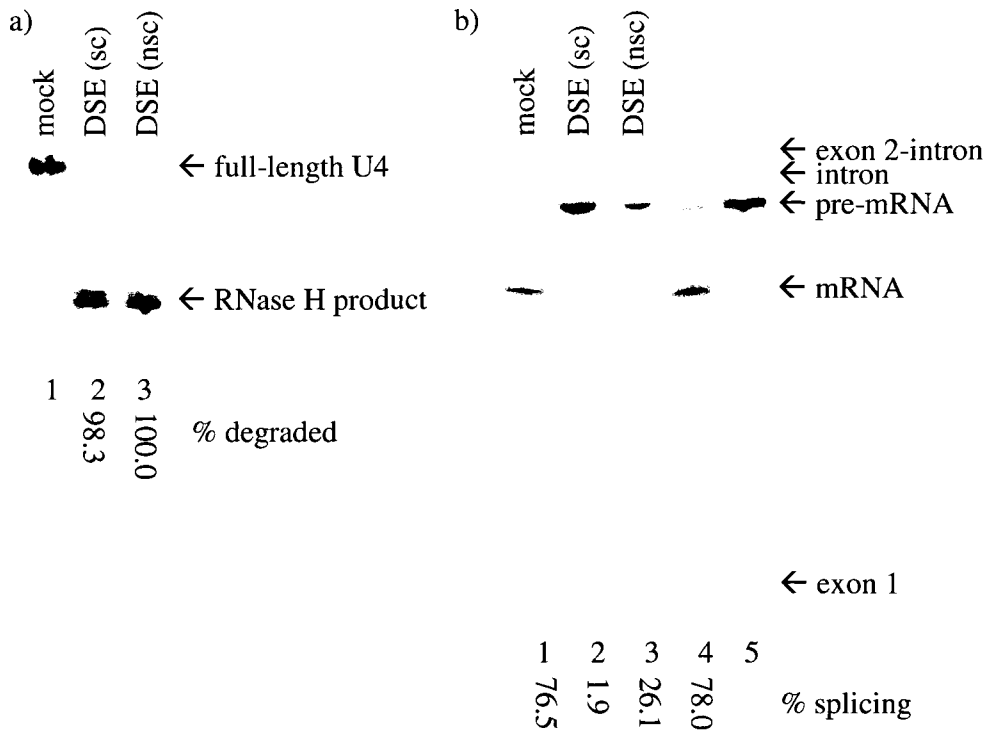

Figure 25. Degradation of the central domain of U4 under splicing conditions, but not non-splicing conditions, blocks subsequent splicing. a) Degradation of U4 in mock-depleted or U4-depleted (DSE) splicing extract by incubation with 0.8 μM U4CM3 (complementary to U4 nucleotides 65 to 88) under splicing (sc) or non-splicing (nsc) conditions. Degradation efficiency is shown below the gel. b) Effect of U4 degradation on subsequent splicing of ^{32}P-labeled actin pre-mRNA. Lanes 4 and 5 are positive and negative splicing controls, respectively. Splicing efficiency of each reaction is shown below the gel.

The lack of reconstitution of di-snRNP formation by U4 mutants lacking the 3′ stem-loop (U4 1-68 and 1-90) was unexpected. This is because reconstitution studies in human nuclear extract and *Xenopus* oocytes have shown that deletion of the Sm-binding site, the 3′ stem-loop, or the entire central domain does not significantly inhibit U4/U6 interaction (Wersig and Bindereif 1990, 1992; Vankan *et al.* 1990). However, the results presented here are consistent with a study by Bordonne *et al.* (1990) in which substitution of the yeast U4 3′ stem-loop by that from *Trypanosoma brucei* U4 snRNA decreased interaction with U6 by

60-70% and was lethal. Similarly, Hu *et al.* (1995) report a deletion within the yeast U4 3′ stem-loop that confers conditional lethality. Together, these results suggest a significant difference between the functionally essential regions of U4 in humans and yeast.

The reason for this apparent requirement of the U4 3′ stem-loop for di-snRNP formation in yeast is unclear. This region of the molecule has not been implicated in protein binding, though limited structural knowledge of the U4 snRNP does not allow exclusion of this possibility. The U4-associated protein Snu13 has been shown to interact directly with the U4 snRNA through the 5′ stem-loop (Nottrott *et al.*1999, Vidovic *et al.* 2000). Similarly, UV cross-linking has indicated that Prp31 contacts U4 nucleotides within and directly upstream of the 5′ stem-loop (Nottrott *et al.*2002). While the putative U4 snRNP protein Prp4 has been shown to require the 5′ region of the snRNA for addition to the di-snRNP (Bordonne *et al.* 1990, Xu *et al.* 1990), direct binding of Prp4 to U4 snRNA has not been demonstrated. As well, the binding site for Prp3, also a potential U4-associated protein (Anthony *et al.* 1997, Ayadi *et al.* 1998), has not yet been identified. It may be that one of these proteins, or another as-yet unidentified splicing factor, interacts with U4 through the 3′ stem-loop, either exclusively or in addition to interaction with the 5′ region of the molecule.

It is also possible that the 3′ stem-loop itself is required for folding of the RNA into the correct secondary structure by preventing formation of competing, non-functional conformations, or that it participates in stabilization of the correct tertiary structure through formation of A-minor interactions with other regions of the molecule. A-minor interactions, involving interaction of a stack of single-stranded nucleotides, usually adenosines, with the minor groove of a helix, are a common form of helix packing in RNA molecules (Daherty *et al.* 2001). Thus, it is possible that interaction of the 3′ stem-loop with a single-stranded,

adenosine-rich region, such as the 3′ portion of the central domain (Figure 3), is required for the subsequent U4 snRNA interactions leading to di-snRNP formation, spliceosome assembly, and splicing. Whatever the function of the 3′ stem-loop in yeast, the dispensability of this domain for splicing in human nuclear extract and *Xenopus* oocytes (Wersig and Bindereif 1992, Vankan 1990) suggests that the function is either not required in these systems or has been replaced by a splicing factor not present in yeast. Future U4 reconstitution analyses will be aimed at investigating the role of the 3′ stem-loop in snRNP formation (see Chapter 5 for further discussion).

CHAPTER 4

Identification of Optimal Conditions for Reconstitution of Functional U6 snRNPs and Generation of U4/U6-Depleted Extract

The development of a system for *in vitro* reconstitution of functional U4 snRNPs , as described in Chapter 3, opens the door to a large number of experiments probing the structure and function of the U4 snRNP. One of the questions which this system may be used to investigate is how formation of the U4/U6 di-snRNP is initiated. As discussed in Section 1.6.1, it has been proposed that these snRNAs first interact through complementary nucleotides located in loop structures at the 5′ end of U4 and the 3′ end of U6 (Figure 3b), initiating formation of stems I and II (Karaduman *et* al. 2006; Ollenberger and Rader, unpublished results). This kissing-loop hypothesis could be tested using *in vitro* reconstitution by first mutating U4's loop residues in a way predicted to block di-snRNP formation, and then reconstituting extract depleted of both U4 and U6 with the mutant U4 and a U6 containing compensatory mutations and examining their ability to base-pair. If the kissing-loop model is correct, and if the mutated residues do not play a role beyond the U4/U6 interaction, di-snRNP formation and splicing activity should be restored. Restoration of the U4/U6 interaction but continued blockage of splicing would still support the kissing-loop model, but would also indicate that the mutated residues play a role beyond initiation of di-snRNP formation. Thus, examination of the kissing-loop hypothesis requires a system for depletion and reconstitution of both U4 and U6 at the same time. To this end, I identified conditions allowing both optimal reconstitution of U6 snRNPs and efficient generation of U4/U6 depleted splicing extract.

4.1 Materials and Methods

4.1.1 RNase H Degradation and Reconstitution of U6

RNase H degradation of U6 was performed as described for U4, except this reaction was not carried out under conditions of active splicing (unlabeled actin pre-mRNA was omitted) and the targeting oligonucleotide used was:

SDR419 (complementary to U6 nucleotides 28 to 54)

5' ATCTCTGTATTGTTTCAAATTGACCAA 3'

Reactions were incubated for 30 minutes at 30°C.

Reconstitution of splicing in U6-depleted splicing extract by IVT U6 was examined as for U4, except that, where indicated, a blocking oligonucleotide complementary to the targeting oligonucleotide was added following RNase H degradation, prior to addition of IVT U6. The sequence of this blocking oligonucleotide was:

SDR588

5' TTTGAAACAATACAG 3'

4.1.2 Generation of U4/U6-Depleted Splicing Extract

Splicing extract depleted of both U4 and U6 was generated by first degrading U4 as described previously and then adding U6 targeting oligo and incubating the reaction for an additional 30 minutes at 30°C. Degradation efficiency was analyzed by Northern blot as described previously.

4.2 Results and Discussion

4.2.1 Optimal Conditions for Reconstitution of Functional U6 snRNPs

A system for *in vitro* reconstitution of functional U6 snRNPs has been described previously (Fabrizio *et al.* 1989). Therefore, I performed initial U6 reconstitution attempts according to this protocol. However, while Fabrizio *et al.* (1989) report efficient reconstitution of splicing with 10nM IVT U6, I did not observe reconstitution with IVT U6 concentrations up to 100nM (Figure 26, lanes 3 and 4). In a more recent study employing *in vitro* reconstitution of functional U6, McGrail *et al.* (2006) report that a blocking oligonucleotide complementary to the targeting oligonucleotide was added to U6-depleted splicing extract prior to addition of IVT U6. I also found that use of a blocking oligonucleotide allowed successful reconstitution of splicing in U6-depleted extract (Figure 26, lanes 5 and 6). However, the level of splicing reconstituted (10-20% compared to the mock-depleted extract) was significantly lower than that reported by Fabrzio *et al.* (1989) (50-100%, using 10nM IVT U6).

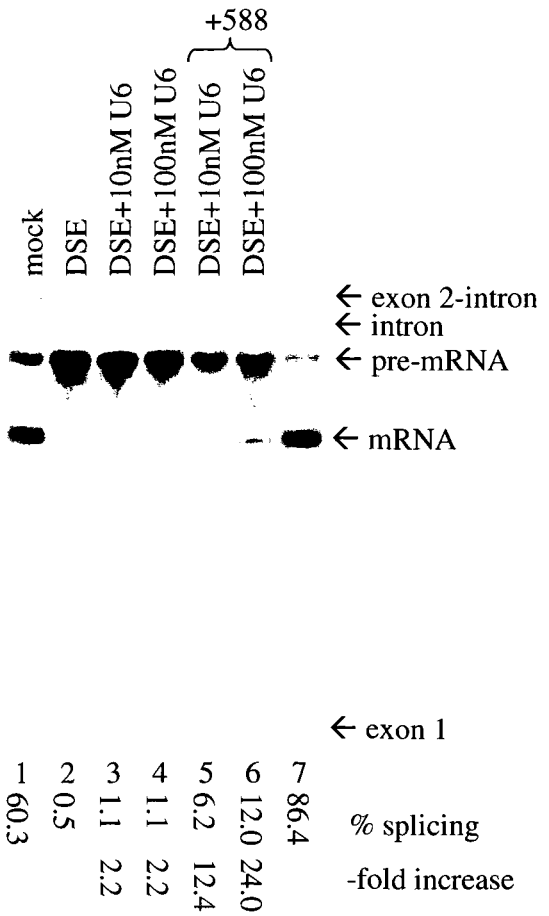

Figure 26. U6 reconstitution requires addition of a blocking oligonucleotide. Splicing in mock depleted (lane 1) or U6-depleted (lanes 2-6) splicing extract in the presence of the indicated concentrations of IVT U6. 1.25μM blocking oligonucleotide (SDR588) was added to reactions 5 and 6 prior to addition of IVT U6. Lane 7 is a positive splicing control. Splicing efficiency and fold increase in splicing upon reconstitution are shown below the gel.

To improve reconstitution of splicing in U6-depleted extract, I investigated lower concentrations of targeting oligonucleotide and higher concentrations of blocking oligonucleotide and IVT U6. Targeting oligonucleotide concentrations below 0.3μM resulted in lower efficiencies of U6 degradation (Figure 27b) and splicing inhibition (Figure 27a), and therefore produced a smaller increase in splicing upon reconstitution. However, increasing the concentration of both the blocking oligonucleotide (Figure 27a, lane 6) and IVT U6

(Figure 27a, lane 8) improved splicing reconstitution from 4.7% to 5.5% and 5.9%, respectively, though still not to the level reported by Fabrizio *et al.* (1989). Further increases in blocking oligonucleotide concentration did not improve splicing reconstitution (data not shown).

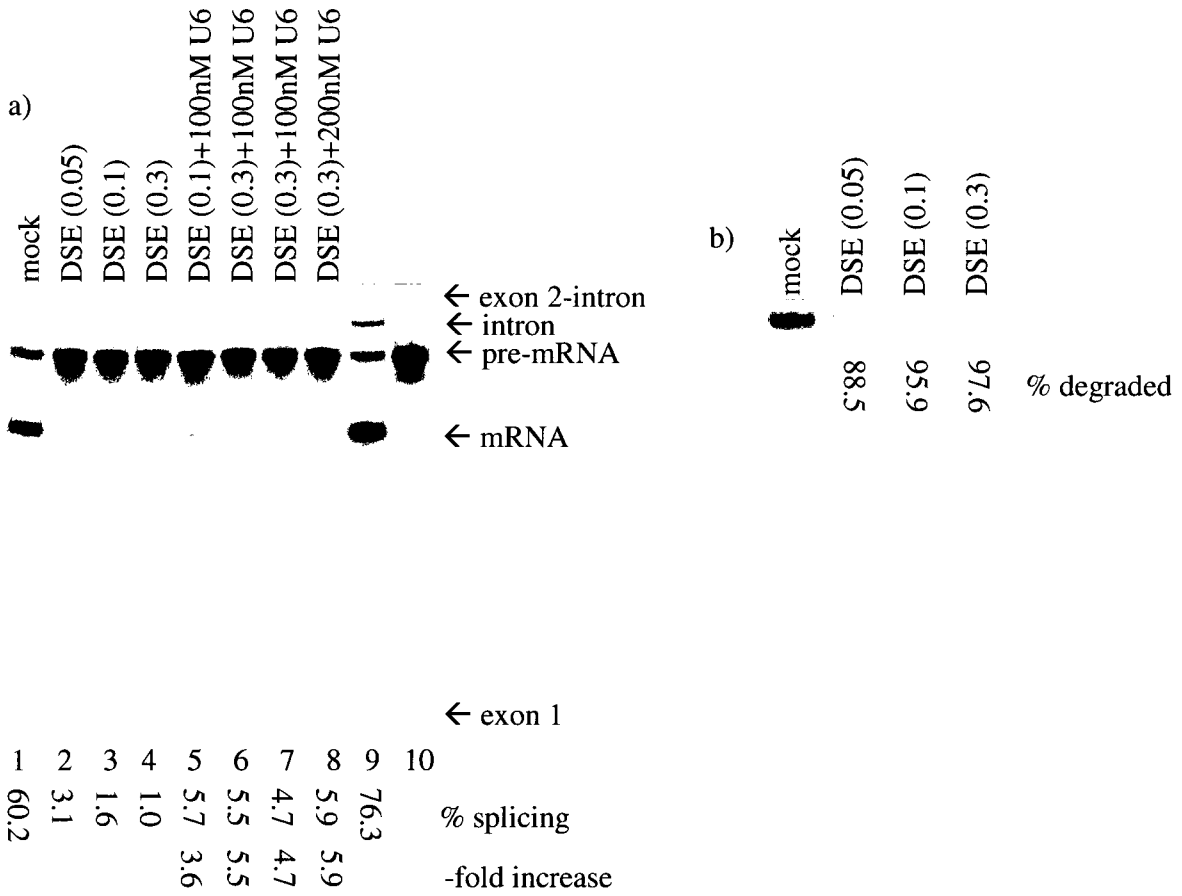

Figure 27. 0.3μM oligonucleotide allows maximal U6 degradation and reconstitution. a) Inhibition of splicing by incubation of extract with 0.05 to 0.3 μM SDR419 and reconstitution of splicing by addition of 100 or 200 nM IVT U6. Blocking oligo was added prior to IVT U6 at 1.25μM (lanes 5, 7, and 8) or 2.5μM (lane 6). Lanes 9 and 10 are positive and negative splicing controls, respectively. Splicing efficiency of each reaction and fold increase in splicing upon reconstitution are shown below the gel. b) Degradation of U6 by incubation of extract with the indicated concentrations of SDR419. Degradation efficiency is shown below the gel.

As efficiency of splicing reconstitution was better with 200μM IVT U6 than 100μM (Figure27a, lanes 7 and 8), I examined the effect of further increases in IVT U6 concentration on reconstitution efficiency. Figure 28a shows that reconstitution by 400nM IVT U6 was approximately equal to that by 500nM but better than that by 300nM or 600nM (data not shown). Splicing reconstitution was further improved by performing a five minute incubation at 23°C between addition of the blocking oligonucleotide and addition of IVT U6 (Figure 28a, lanes 7 and 8). In summary, maximum reconstitution of splicing in U6-depleted extract was achieved by adding 2.5μM blocking oligonucleotide, incubating the reaction for five minutes at 23°C, then adding 400nM IVT U6. These conditions yielded a splicing efficiency of 14.9%, an approximately 10-fold increase over the U6-depleted extract.

Splicing reconstitution efficiency in U6-depleted extract also varied substantially depending on the extract preparation used (Figure 28a, lanes 5-7). This variation was not due to differences in U6 degradation, since, as shown in Figure 28b, U6 degradation was nearly equal in the three extracts, resulting in similarly close levels of splicing inhibition (Figure 28a, lanes 2-4). Differences in the concentrations of U6-specific proteins or endogenous nucleases may have contributed to the observed extract-specific reconstitution efficiencies.

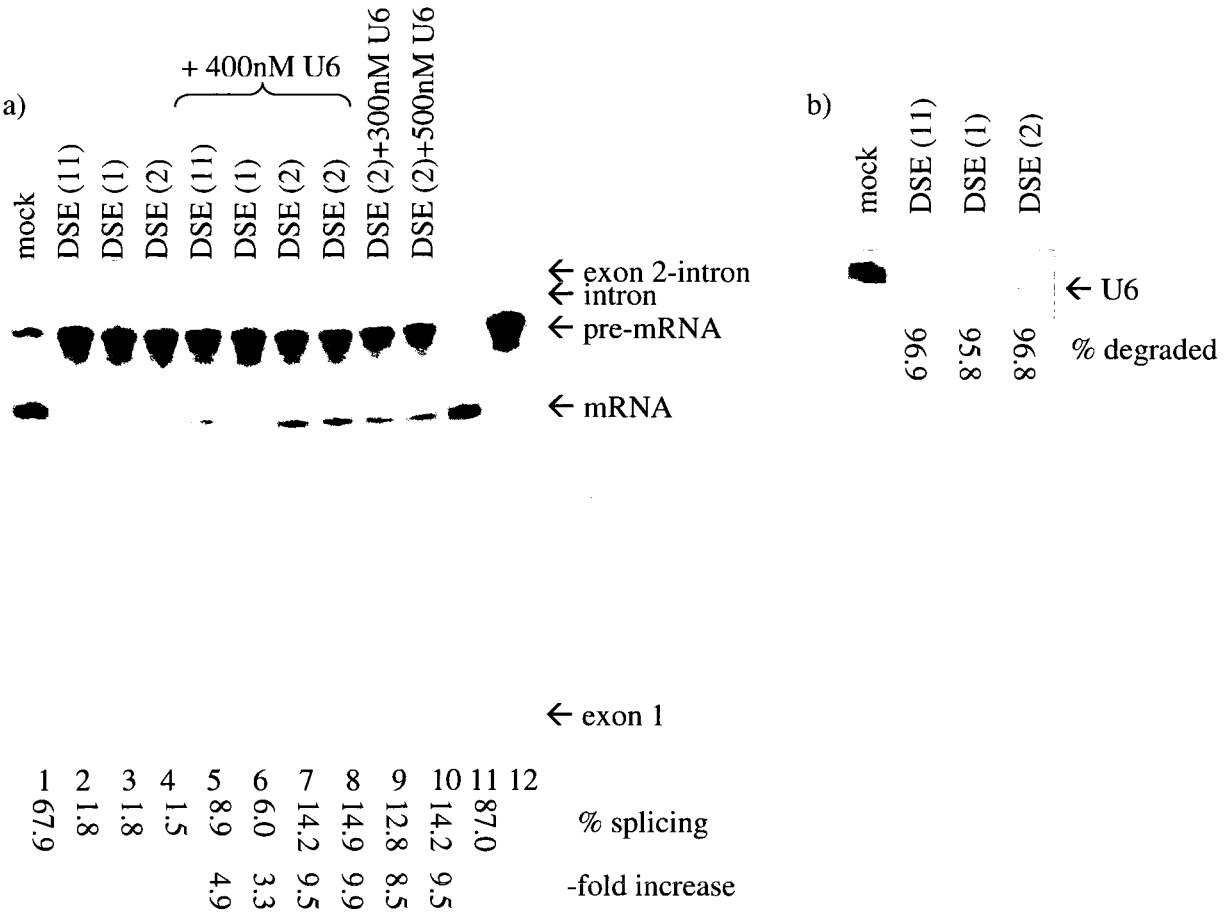

Figure 28. U6 Reconstitution efficiency is extract dependent. a) Inhibition of splicing in three different extracts (11, 1, and 2) and reconstitution of splicing by addition of 300 to 500nM IVT U6. Reaction 8 had a five minute incubation at 23°C between addition of 2.5μM blocking oligonucleotide and IVT U6. Lanes 11 and 12 are positive and negative splicing controls, respectively. Splicing efficiency and fold increase in splicing upon reconstitution are shown below the gel. b) Northern blot showing degradation of endogenous U6 in each of the extracts.

4.2.2 Generation of U4/U6-Depleted Splicing Extract

Investigation of the kissing-loop hypothesis requires generation of extract depleted of both U4 and U6. While U4 degradation must be performed under conditions of active splicing (Figures 5 and 6), U6 degradation is greatly inhibited by such conditions (Figure

29a). This suggests that, upon incorporation of U6 into the active spliceosome, the targeted region of U6, nucleotides 28-54, becomes protected from binding by the targeting oligonucleotide and subsequent degradation by RNase H. Given that the 3' portion of the targeted sequence contains the ACAGAGA sequence that binds to the 5' splice site in the active spliceosome, it is likely that this competition for binding of the target sequence, as well as steric hindrance from surrounding spliceosomal components, inhibited binding of the targeting oligonucleotide and degradation by RNase H. I successfully generated U4/U6 depleted extract by sequential degradation of U4 (under splicing conditions) followed by U6 (under non-splicing conditions due to U4 degradation) (Figure29b and c). Similarly, it should be possible to follow degradation of U6 under non-splicing conditions by degradation of U4, since the prior degradation of U6 should have released U4 into the free snRNP species which is accessible to its targeting oligonucleotide. These two approaches will be compared in future experiments examining the efficiencies of splicing inhibition and reconstitution in U4/U6-depleted extract.

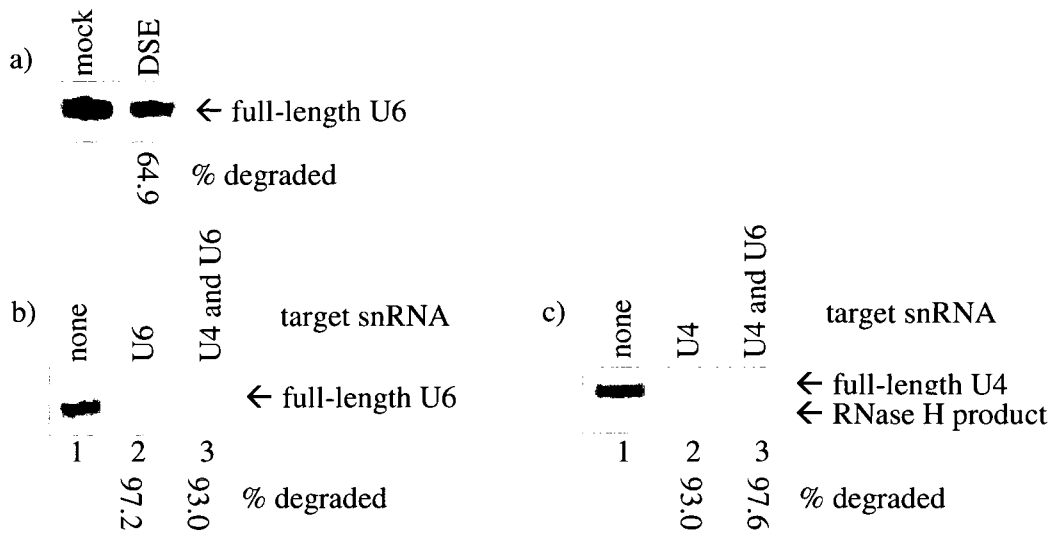

Figure 29. U6 degradation efficiency is decreased under conditions of active splicing. a) Northern blot showing degradation of U6 under conditions of active splicing. b) and c) Northern blot showing degradation of b) U6 and c) U4 either alone (lane 2) or by sequential degradation of U4 followed by U6 (lane 3). Degradation efficiency is shown below the gels.

CHAPTER 5

Future Directions

Successful development of a U4 *in vitro* reconstitution system opens to door to a wide array of experiments exploring the effects of specific mutations in U4 on its ability to interact with other spliceosomal components and to participate in the splicing reaction. Such experiments will play a key role in defining the structure and function of the U4 snRNP, thus contributing to our overall understanding of the mechanism by which pre-mRNA splicing is accomplished.

5.1 Identification of U4 snRNP Proteins and Their snRNA Binding Sites

As discussed above in Section 3.2.2.2, our knowledge of the identities of the proteins associated with U4 snRNA, the RNA sequences to which they bind, and their functions in spliceosome assembly and splicing is rather limited. While the list of putative U4-associated proteins includes Snu13, Prp3, Prp4, and Prp31, direct binding to U4 has been demonstrated by crystal structure determination or UV cross-linking for only Snu13 and Prp31 (Nottrott *et al.* 1999, Vidovic *et al.* 2000, Nottrott *et al.* 2002). Furthermore, these analyses were performed using only fragments of the 5′ portion of U4 snRNA, so that any interactions of these proteins with 3′ regions of the molecule would have gone undetected.

The U4 *in vitro* reconstitution assay presented here provides a useful technique for further investigation of the protein complement of the U4 snRNP. By reconstituting U4-depleted extract with ^{32}P-labeled IVT U4, assembly of the U4 snRNP can be visualized using non-denaturing gel electrophoresis. We have found that depletion of U6 prevents assembly of the reconstituted U4 snRNPs into di- or tri-snRNPs, resulting in a clear accumulation of the

free U4 snRNP (data not shown). By using yeast strains in which individual potential U4-associated proteins have been labeled with a TAP tag, this reconstitution assay could then be used to investigate the protein components of the U4 snRNP through antibody supershift analysis. Such an experiment may even shed light on the temporal organization of snRNP assembly. Initial investigation of U4 snRNP assembly has suggested that this process occurs in a stepwise manner, as indicated by the appearance of multiple lower bands below the fully assembled U4 snRNP (data not shown). Identification of the proteins present in each band through supershift analysis could therefore contribute to our understanding of the relative timing of the interactions involved in U4 snRNP assembly.

To further elucidate the interactions involved in U4 snRNP assembly, antibody supershift analysis could be performed in extract reconstituted with mutant U4 snRNAs. Individual deletion or point mutations could thereby be linked to disruption of the association of specific proteins, providing insight into the regions of the snRNA that are required for the binding of these proteins, either directly or through another splicing factor.

Supershift analysis of a U4 3′ stem-loop deletion mutant would be particularly interesting, since, by identifying any protein factors requiring this region for association with U4, such an experiment may clarify why this domain is essential for di-snRNP formation in yeast. As a mutational analysis of yeast U4 identified deletion of nucleotides 131-133 as the only mutation in the 3′ stem-loop that affected growth (Hu *et al.* 1995), performing supershift analysis with this mutant may assist in pinpointing the sequence in the 3′ stem-loop required for any protein associations.

Another useful technique for identifying U4 snRNA interaction partners that is made possible by the availability of a U4 *in vitro* reconstitution assay is formation of specific

cross-links between U4 snRNA and other spliceosomal components. By reconstituting with 4-thiouridine-labeled U4, this procedure would allow mapping of the interactions of individual U4 nucleotides. Placement of a 4-thiouridine residue near nucleotides 131-133 may be particularly informative for determining the essential function of the 3′ stem-loop.

5.2 Analysis of Formation of the U4/U6 di-snRNP

Development of a U4 *in vitro* reconstitution assay also facilitates investigation of the mechanism of U4/U6 di-snRNP formation. As discussed in Section 1.6.1, it has been proposed that these snRNAs first interact through complementary nucleotides located in loop structures at the 5′ end of U4 and the 3′ end of U6 (Figure 3b), initiating formation of stems I and II (Karaduman *et* al. 2006; Ollenberger and Rader, unpublished results). To test this so-called kissing-loop model of U4/U6 interaction, site-directed mutagenesis could be used to generate specific U4 and U6 mutants. Reconstitution of U4-depleted extract with U4 snRNA mutated at nucleotides 7-10, the 5′ loop residues, would allow examination of the prediction that disruption of the putative loop-loop interaction would block U4/U6 base-pairing and splicing. Using extract that has been co-depleted of U4 and U6 using the protocol described in Section 4.2.2, U4/U6 base-pairing and splicing activity could then be analyzed following reconstitution with the U4 mutant and a U6 mutant containing compensatory base changes in its putative kissing-loop sequence. If the kissing-loop model is correct, and if the mutated residues do not play a role beyond the U4/U6 interaction, di-snRNP formation and splicing activity would be restored. Restoration of the U4/U6 interaction but continued blockage of splicing would still support the kissing-loop model, but would also indicate that the mutated residues play a role beyond initiation of di-snRNP formation.

A second aspect of U4/U6 di-snRNP formation that may be illuminated using the U4 *in vitro* reconstitution assay concerns the function of the splicing factor Prp24. As previously discussed, this protein is thought to catalyze U4/U6 annealing, but it is not clear if its role is limited to di-snRNP formation, or whether it also performs an additional function later in spliceosome assembly by promoting the unwinding of the U4/U6 duplex required for formation of the active spliceosome (Ghetti *et al.* 1995, Raghunathan and Guthrie 1998, Vidaver *et al.* 1999). If the function of Prp24 is indeed limited to promotion of U4/U6 annealing by bringing these snRNAs into close proximity, then association of the snRNAs through an alternative means would be expected to eliminate the requirement for Prp24. One possible approach to investigate this question is to fuse the U4 and U6 snRNAs and look at weather this hybrid molecule is able to reconstitute splicing in U4/U6-depleted extract. If the fused snRNAs are functional, then examination of splicing reconstitution in extract immunodepleted of Prp24 would reveal whether this mutation makes Prp24 redundant. If Prp24 is dispensable in this system, then only an early, duplex-forming role for Prp24 would be supported, whereas lack of splicing reconstitution by the fused snRNAs in the absence of Prp24 would indicate that either the snRNAs are unable to base-pair without Prp24, or that the U4/U6 duplex is formed, but Prp24 is required for progression to the active spliceosome. Together, these experiments would help define the complex and dynamic network of interactions involved in pre-mRNA splicing.

Literature Cited

Alvi, R., Lund, M., and O'Keefe, R. 2001. ATP-dependent interaction of yeast U5 snRNA loop 1 with the 5′ splice site. RNA 7:1013-1023.

Ambion MEGAshortscript™ Kit Handbook, July 2008.

Ansari, A. and Schwer, B. 1995. SLU7 and a novel activity, SSF1, act during the PRP16-dependent step of yeast pre-mRNA splicing. EMBO Journal 14:4001-4009.

Anthony, J., Weidenhammer, E., and Woolford, J. 1997. The yeast Prp3 protein is a U4/U6 snRNP protein necessary for integrity of the U4/U6 snRNP and the U4/U5.U5 tri-snRNP. RNA 3:1143-1152.

Ayadi, L., Callebaut, I., Saguez, C., Villa, T., Mornon, J., and Banroques, J. 1998. Functional and structural characterization of the Prp3 binding domain of the yeast Prp4 splicing factor. Journal of Molecular Biology 284:673–687.

Behzadnia, N., Hartmuth, K., Will, C., and Luhrmann, R. 2006. Functional spliceosomal A complexes can be assembled *in vitro* in the absence of a penta-snRNP. RNA 12:1738-1746.

Berget, S., Moore, C., and Sharp, P. 1977. Spliced segments at the 5' terminus of adenovirus 2 late mRNA. Proceedings of the National Academy of Science 74:3171-3175.

Berget, S. and Robberson, B. 1986. U1, U2, and U4/U6 small nuclear ribonucleoproteins are required for in vitro splicing but not polyadenylation. Cell 46:691-696.

Bindereif, A., Wolff, T., and Green, M. 1990. Discrete domains of human U6 snRNA required for the assembly of U4/U6 snRNP and splicing complexes. EMBO Journal 9:251-255.

Black, D. and Steitz, J. 1986. Pre-mRNA splicing in vitro requires intact U4/U6 small nuclear ribonucleaoprotein. Cell 46:697-704.

Black DL. 2003. Mechanisms of alternative pre-messenger RNA splicing. Annual Review of Biochemistry 72:291–336.

Bordonne, R., Banroques, J., Abelson, J., and Guthrie, C. 1990. Domains of yeast U4 spliceosomal RNA required for PRP4 protein binding, snRNP-snRNP interactions, and pre-mRNA splicing in vivo. Genes and Development 4:1185-1196.

Brow, D. and Guthrie, C. 1988. Spliceosomal RNA U6 is remarkably conserved from yeast to mammals. Nature 334:213-218.

Brow, D. and Guthrie, C. 1989. Splicing a spliceosomal RNA. Nature 337:14-15.

Buratti, E., Baralle, M., and Baralle, F. 2006. Defective splicing, disease and therapy: searching for master checkpoints in exon definition. Nucleic Acids Research 34:3494-3510.

Burset M, Seledtsov IA, Solovyev VV. 2000. Analysis of canonical and non-canonical splice sites in mammalian genomes. Nucleic Acids Res 28:4364–4375.

Cheng, S. and Abelson, J. 1987. Spliceosome assembly in yeast. Genes and Development 1:1014-1027.

Chow, L., Gelinas, R., Broker, T., and Roberts, R. 1977. An amazing sequence arrangement at the 5' ends of adenovirus 2 messenger RNA. Cell 12: 1-8.

Daherty, E., Batey, R., Masquida, B., and Doudna, J. 2001. A universal mode of helix packing in RNA. Nature Structural. Biology 8:339–343.

Davis, C., Grate, L., Spingola, M., and Ares M. 2000. Test of intron predictions reveals novel splice sites, alternatively spliced mRNAs and new introns in meiotically regulated genes of yeast. Nucleic Acids Research 28: 1700–1706.

Dix, I., Russell, C., O'Keffe, R., Newman, A., and Beggs, J. 1998. Protein-RNA interaction in the U5 snRNP of *Saccharomyces cerevisiae*. RNA 4:1239-1250.

Fabrizio, P., McPheeters, D., and Abelson, J. 1989. *In vitro* assembly of yeast U6 snRNP: a functional assay. Genes and Development 3:2137-2150.

Fabrizio, P. and Abelson, J. 1990. Two domains of yeast U6 small nuclear RNA required for both steps of nuclear precursor messenger RNA splicing. Science 250:404-409.

Faustino, N. and Cooper, T. 2003. Pre-mRNA splicing and human disease. Genes and Development. 17:419-437.

Fischer, U., Sumpter, V., Sekine, M., Satoh, T., and Luhrmann, R. 1993. Nucleo-cytoplasmic transport of UsnRNPs: definition of a nuclear localization signal in the Sm core domain that binds a transport receptor independently of the m3G cap. EMBO Journal 12:573-583.

Fortner, D., Troy, R., and Brow, D. 1994. A stem/loop in U6 RNA defines a conformational switch required for pre-mRNA splicing. Genes and Development 8:221-233.

Ghetti, A., Company, M., and Abelson, J. 1995. Specificity of Prp24 binding to RNA: A role for Prp24 in the dynamic interaction of U4 and U6 snRNAs. RNA 1:132-145.

Goffeau, A., Barrell, B., Bussey, B. *et al.* 1996. Life with 6000 genes. Science 274:546-567.

Guthrie, C. and Patterson, B. 1988. Spliceosomal snRNAs. Annual Review of Genetics 22:387-419.

Hall, S. and Padgett R. 1994. Conserved sequences in a class of rare eukaryotic nuclear introns with non-consensus splice sites. Journal of Molecular Biology 239:357–365.

Hamm, J., Kazmaier, M., and Mattaj, I. 1987. In vitro assembly of U1 snRNPs. EMBO Journal. 6:3479-3485.

Hamm, J., Santen, V., Spritz, R., and Mattaj, I. 1988. Loop I of U1 small nuclear RNA is the only essential RNA sequence for binding of specific U1 small nuclear ribonucleoprotein particle proteins. Molecular and Cellular Biology 8:4787-4791.

Hamm, J., Dathan, N., Scherly, D., and Mattaj, I. 1990. Multiple domains of U1 snRNA, includingU1 specific protein binding sites, are required for splicing. EMBO Journal. 9:1237-1244.

Harrison, P., Kumar, A., Lang, N., Snyder, M., and Gerstein, M. 2002. A question of size: the eukaryotic proteome and the problems in defining it. Nucleic Acids Research 30:1083–1090.

Hashimoto, C. and Steitz, J. 1984. U4 and U6 snRNAs coexist in a single small nuclear ribonucleoprotein particle. Nucleic Acids Research 12:3283-3293.

Horowitz, D. and Abelson, J. 1993. A U5 small nuclear ribonucleoprotein particle protein involved only in the second step of pre-mRNA splicing in *Saccharomyces cerevisiae*. Molecular and Cellular Biology 13:2959-2970.

Hu, J., Deming, X., Schappert, K., Xu, Y., and Friesen, J. 1995. Mutational analysis of *Saccharomyces cerevisiae* U4 small muclear RNA identifies functionally important domains. Molecular and Cellular Biology 15:1274-1285.

Huang, J., Brieba, L., and Sousa, R. 2000. Misincorporation by wild-type and mutant T7 RNA polymerases: identification of interactions that reduce misincorporation rates by stabilizing the catalytically incompetent open conformation. Biochemistry 39:11571-11580.

Huppler, A., Nikstad, L., Allmann, A., Brow, D., and Butcher, S. 2002. Metal binding and base ionization in the U6 RNA intramolecular stem-loop structure, Nature Structural Biology 9:431–435.

Johnson, T. and Abelson, J. 2001. Characterization of U4 and U6 interactions with the 5' splice site using a *S. cerevisiae* in vitro *trans*-splicing system. Genes and Development. 15:1957–1970

Johnson, J., Castle, J., Garrett-Engele, P., Kan, Z., Loerch, P., Armour, C., Santos, R., Schadt, E., Stoughton, R., and Shoemaker, D. 2003. Genome-wide survey of human alternative pre-mRNA splicing with exon junction microarrays. Science 302:2141-2144.

Karaduman, R., Fabrizio, P., Hartmuth, K., Urlaub, H., and Lührmann, R. 2006. RNA Structure and RNA-Protein Interactions in Purified Yeast U6 snRNPs. Journal of Molecular Biology 356:1248-1262.

Kleinschmidt, A., Patton, J., and Pederson, T. 1989. U2 small nuclear RNP assembled in vitro. Nucleic Acids Research. 17:4817-4828.

Krummel, D., Oubridge, C., Leung, A., Li,. J., and Nagai, K. 2009. Crystal structure of human spliceosomal U1 snRNP at 5.5 Å resolution. Nature 458:475-480.

Lamond, A., Konarska, M., Grabowski, P., and Sharp, P. 1988. Spliceosome assembly involves the binding and release of U4 small nuclear ribonucleoprotein. Proceedings of the National Academy of Science 85:411-415.

Lamond, A. and Sproat, B. 1994. Targeted RNase H cleavage of RNA. In: RNA Processing: A Practical Approach. 123-126.

Lander, E., Linton, L., Birren, B., *et al.* 2001. Initial sequencing and analysis of the human genome. Nature 409:860-921.

Li, Z. and Brow, D. 1993. A rapid assay for quantitative detection of specific RNAs. Nucleic Acids Research 21:4645-4646.

Lin, R., Newman, A., Cheng, S., and Abelson, J. 1985. Yeast mRNA splicing in vitro. Journal of Biological Chemistry 260:14780-14792.

Lopez-Bigas, N., Audit, B., Ouzounis, C., Parra, G., and Guigo, R. 2005. Are splicing mutations the most common cause of hereditary disease? FEBS Letters 579:1900-1903.

Luo, H., Moreau, G., Levin, N., and Moore, M. 1999. The human Prp8 protein is a component of both U2- and U12-dependent spliceosomes. RNA 5:893-908.

Madhani, H. and Guthrie, C. 1992. A novel base-pairing interaction between U2 and U6 snRNAs suggests a mechanism for the catalytic activation of the spliceosome, Cell 71:803–817.

McConnell, T. and Steitz, J. 2001. Proximity of the invariant loop of U5 snRNA to the second intron residue during pre-mRNA splicing. EMBO Journal 20:3577-3586.

McGrail, J., Tatum, E., and O'Keefe, R. 2006. Mutation in the U2 snRNA influences exon interactions of U5 snRNA loop 1 during pre-mRNA splicing. EMBO Journal 25:3813-3822.

McPheeters, D., Fabrizio, P., and Abelson, J. 1989. *In vitro* reconstitution of functional yeast U2 snRNPs. Genes and Development 3:2124-2136.

Miesfeld, R. 1999. Using yeast as a model eukaryotic cell In: Applied Molecular Genetics. Wiley-Liss Toronto.

Myslinski, E. and Branlant, C. 1991. A phylogenetic study of U4 snRNA reveals the existence of an evolutionarily conserved secondary structure corresponding to "free" U4 snRNA. Biochimie 73:17-28.

Murray, H. and Jarrell, K. 1999. Flipping the switch to an active spliceosome. Cell 96:599-602.

Newman, A. 1994. Depletion of components from splicing extract. In: RNA Processing: A Practical Approach. 193-194.

Nilsen, T. 1994. RNA–RNA interactions in the spliceosome: unraveling the ties that bind. Cell 78:1–4.

Nottrott, S., Hartmuth, K., Fabrizio, P., Urlaub, H., Vidovic, I., Ficner, R., and Luhrmann, R. 1999. Functional interaction of a novel 15.5kD [U4/U6.U5] tri-snRNP protein with the 5′ stem-loop of U4 snRNA. EMBO Journal 18:6119-9133.

Nottrott, S., Urlaub, H., and Luhrmann, R. 2002. Hierarchical, clustered protein interactions with U4/U6 snRNA: a biochemical role for U4/U6 proteins. EMBO Journal 21:5527-5538.

O'Keefe, R., Norman, C., and Newman, A. 1996. The invariant U5 loop 1 sequence is dispensible for the first catalytic step of pre-mRNA splicing in yeast. Cell 86:679-689.

O'Keefe, R. and Newman, A. 1998. Functional analysis of the U5 snRNA loop 1 in the second catalytic step of yeast pre-mRNA splicing. EMBO Journal 17:565-574.

Patton, J., Patterson, R., and Pederson, T. 1987. Reconstitution of the U1 small nuclear ribonucleoprotein particle. Molecular and Cellular Biology. 7:4030-4037.

Patton, J. and Pederson, T. 1988. The Mr70,000 protein of the U1 small nuclear ribonucleoprotein particle binds to the 5′ stem-loop of U1 RNA and interacts with Sm domain proteins. Proceedings of the National Academy of Sciences 85:747-751.

Pikielny, C., Rymond, B., and Rosbash, M. 1986. Electrophoresis of ribonucleoproteins reveals an ordered assembly pathway of yeast splicing complexes. Nature 324:341-345.

Pikielny, C., Bindereif, A., and Green, M. 1989. In vitro reconstitution of snRNPs: a reconstituted U4/U6 snRNP participates in splicing complex formation. Genes and Development 3:479-487.

Raghunathan, P. and Guthrie, C. 1998. A spliceosomal recycling factor that reanneals U4 and U6 small nuclear ribonucleoprotein particles. Science 279:857-860.

Reyes, V., and Abelson, J. 1988. Substrate recognition and splice site determination in yeast tRNA splicing. Cell 55:719-730.

Riedel, N., Wolin, S., and Guthrie, C. 1987. A subset of yeast snRNAs contains functional binding sites for the highly conserves Sm antigen. Science 235:328-331.

Rinke, J., Appel, B., Digweed, M. and Lührmann, R. 1985. Localization of a base-paired interaction between small nuclear RNAs U4 and U6 in intact U4/U6 ribonucleoprotein particles by psoralen cross-linking. Journal of Molecular Biology 185:721-731.

Ryan, D., Stevens, S., and Abelson, J. 2002. The 5' and 3' Domains of Yeast U6 snRNA: Lsm Proteins Facilitate Binding of Prp24 Protein to the U6 Telestem Region. RNA 8:1011-1033.

Rymond, B. and Rosbash, M. 1986. Differential nuclease sensitivity identifies tight contacts between yeast pre-mRNA and spliceosomes. EMBO Journal 5:3517-3523.

Rymond, B. and Rosbash, M. 1992. Yeast pre-mRNA splicing. In: The Molecular and Cellular Biology of the Yeast Saccharomyces: Gene Expression. 143–192.

Segault, V., Will, C., Sproat, B., and Luhrmann, R. 1995. *In vitro* reconstitution of mammalian U2 and U5 snRNPs active in splicing: Sm proteins are functionally interchangeable and are essential for the formation of functional U2 and U5 snRNPs. EMBO Journal 14:4010-4021.

Sumpter, V., Kahrs, A., Fischer, U., Kornstadt, U., and Luhrmann, R. 1992. In vitro reconstitution of U1 and U2 snRNPs from isolated proteins and snRNA. Molecular Biology Reports. 16:229-240.

SGD project. 1997. "Saccharomyces Genome Database" <www.yeastgenome.org> Accessed May 2008.

Siliciano, P., Brow, D., Roiha, H., and Guthrie, C. 1987. An essential snRNA from *S. cerevisiae* has properties predicted for U4, including interaction with a U6-like snRNA. Cell 50:585-592.

Staley, J. and Guthrie. C. 1998. Mechanical devices of the spliceosome: motors, clocks, springs, and things. Cell 92:315-26.

Stevens, S., Ryan, D., Ge, H., Moore, R., Young, M., Lee, T., and Abelson, J. 2002. Composition and functional characterization of the yeast spliceosomal penta-snRNP. Molecular Cell 9:31-44.

Umen, J. and Guthrie, C. 1995. The second catalytic step of pre-mRNA splicing. RNA 1:869-885.

Vankan, P., McGuigan, C., and Mattaj, I. 1990. Domains of U4 and U6 snRNAs required for snRNP assembly and splicing complementation in *Xenopus* oocytes. EMBO Journal 9:3397-3404.

Vankan, P., McGuigan, C., and Mattaj, I. 1992. Roles of U4 and U6 snRNAs in the assembly of splicing complexes. EMBO Journal 11:335-343.

Vidal, V., Verdone, L., Mayes, A., and Beggs, J. 1999. Characterization of U6 snRNA-protein interactions. RNA 5:1470-1481.

Vidaver, R., Fortner, D., Loos-Austin, L., and Brow, D. 1999. Multiple functions of Saccharomyces cerevisiae splicing protein Prp24 in U6 RNA structural rearrangements. Genetics 153:1205-1218.

Vidovic, I., Nottrott, S., Hartmuth, K., and Luhrmann, R. 2000. Crystal structure of the spliceosomal 15.5kDprotein bound to a U4 snRNA fragment. Molecular Cell 6:1331-1342.

Wersig, C., and A. Bindereif. 1990. Conserved domains of human U4 snRNA required for snRNP and spliceosome assembly. Nucleic Acids Res. 18:6223-6229.

Wersig, C. and Bindereif, A. 1992. Reconstitution of functional mammalian U4 small nuclear ribonucleoprotein: Sm protein binding is not essential for splicing. Molecular and Cellular Biology 12:1460-1468.

Will, C., Rumpler, S., Gunnewiek, J., Venrooij, W., and Luhrmann, R. 1996. *In vitro* reconstitution of mammalian U1 snRNPs active in splicing: the U1-C protein enhances the formation of early (E) spliceosomal complexes. Nucleic Acids Research 24:4614-4623.

Wolff, T. and Bindereif, A. 1992. Reconstituted mammalian U4/U6 snRNP complements splicing: a mutational analysis. EMBO Journal 11:345-359.

Wolff, T., Menssen, R., Hammel, J., and Bindereif, A. 1994. Splicing function of mammalian U6 small nuclear RNA: conserved positions in central domain and helix I are essential during the first and second step of pre-mRNA splicing. Proceedings of the National Academy of Science USA 91:903–907.

Xu, Y., Petersen-Bjorn, S., and Friesen, J. 1990. The PRP4 (RNA4) protein of *Saccharomyces cerevisiae* is associated with the 5' portion of the U4 small nuclear RNA. Molecular and Cellular Biology 10:1217-1225.

Yean, S. and Lin, R. 1991. U4 small nuclear RNA dissociates from a yeast spliceosome and does not participate in the subsequent splicing reaction. Molecular and Cellular Biology 11:5571–5577.

Yean, S., Wuenschell, G., Termini, J., and Lin, R. 2000. Metal-ion coordination by U6 small nuclear RNA contributes to catalysis in the spliceosome. Nature 408:881-884.